(Amino)cyclophosphazenes as multisite ligands for the synthesis of antitumoral and antibacterial silver(I) complexes

Elena Gascón [a], *Sara Maisanaba* [b], *Isabel Otal* [c], *Eva Valero* [d], *Guillermo Repetto* [b], *Peter G. Jones* [e], *Josefina Jiménez* *[a]

[a] Dr. J. Jiménez, E. Gascón.

Departamento de Química Inorgánica, Facultad de Ciencias, Instituto de Síntesis Química y Catálisis Homogénea (ISQCH), Universidad de Zaragoza-C.S.I.C., Pedro Cerbuna 12, 50009 Zaragoza (Spain). E-mail: jjimvil@unizar.es

[b] Dr. S. Maisanaba, Dr. G. Repetto.

Departamento de Biología Molecular e Ingeniería Bioquímica, Área de Toxicología, Universidad Pablo de Olavide, Ctra. Utrera, Km 1, Sevilla (Spain).

[c] Dr. I. Otal.

Grupo de Genética de Micobacterias, Departamento de Microbiología, Medicina Preventiva y Salud Pública, Universidad de Zaragoza, Zaragoza (Spain). CIBER de Enfermedades Respiratorias, Instituto de Salud Carlos III, E-28029 Madrid (Spain).

[d] Dr. E. Valero.

Departamento de Biología Molecular e Ingeniería Bioquímica, Área Nutrición y Bromatología, Universidad Pablo de Olavide, Ctra. Utrera, Km 1, Sevilla (Spain).

[e] Prof. P.G. Jones

Technische Universität Braunschweig, Institut für Anorganische und Analytische Chemie, Hagenring 30, D-38106, Braunschweig (Germany).

Keywords: antibacterial, antibiotics, antimicrobial, antitumor agents, phosphazenes, structure-activity relationships, silver.

Abstract

The reactivity of the multi-site (amino)cyclotriphosphazenes ligands, $[N_3P_3(NHCy)_6]$ and $[N_3P_3(NHCy)_3(NMe_2)_3]$, has been explored in order to obtain silver(I) metallophosphazenes complexes. Two series of cationic silver(I) metallophosphazenes were obtained and characterised: $[N_3P_3(NHCy)_6\{AgL\}_n](TfO)_n$ (n=2, L= PPh_3 (**2**), PPh_2Me(**4**); n=3, L= PPh_3 (**3**), PPh_2Me(**5**), TPA(**6**)) and *nongem-trans*-$[N_3P_3(NHCy)_3(NMe_2)_3\{AgL\}_n](TfO)_n$ (n=2, L= PPh_3 (**7**), PPh_2Me(**9**); n=3, L= PPh_3 (**8**), PPh_2Me(**10**)). **5**, **7** and **9** have also been characterised by single-crystal X-ray diffraction,

thereby allowing key bonding information to be obtained. Compounds **2**-**6**, **9** and **10** were screened for the *in vitro* cytotoxic activity against two tumour human cell lines, MCF7 (breast adenocarcinoma) and HepG2 (hepatocellular carcinoma) and for antimicrobial activity against five bacterial species including Gram-positive, Gram-negative and Mycobacteria strains. Both IC_{50} and MIC values revealed an excellent biologic activity for these metal complexes, compared with their precursors and cisplatin, and $AgNO_3$ and silver sulfadiazine, respectively. Both IC_{50} and MIC values are among the lowest values found for any silver derivatives against the cell lines and bacterial strains used in this work. The structure-activity relationships were clear, being the most cytotoxic and antimicrobial derivatives those with triphenylphosphane and $[N_3P_3(NHCy)_6]$ ligands, and with greater number of silvers.

1. Introduction

Over the years, there has been continuous interest in the biological activity of metal complexes. Among them, silver has been used for numerous medical conditions, mostly due to its antibacterial activity. [1] The antibacterial, antifungal and antiviral properties of silver ions, silver compounds and, recently, silver nanoparticles have been extensively studied and these topics have been thoroughly reviewed. [2, 3] Nowadays the preparation of novel antibacterial agents has become a priority due to the presence of multidrug resistant pathogens. [4] *Mycobacterium tuberculosis* (the organism causing tuberculosis that still wreak havoc both in developed and undeveloped countries) aside, *Staphylococcus aureus* (resistant to methicillin, MRSA), *Escherichia coli* and *Pseudomonas aeruginosa*, among others, are becoming more and more resistant and the lack of efficient treatment is one of the leading causes of high mortality rates. [5] Although the antimicrobial activity mechanism of silver (I) complexes has not been well established, [2a, 6] microorganisms are unlikely to develop resistance against silver as compared to antibiotics since silver attacks a broad range of targets in the microbes, and only a few accounts of resistance have been reported. [7] What is more, silver is also found to be non-toxic to humans in minute concentrations. [8] The most widely used silver reagents have been in the form of inorganic salts or complexes, such as silver nitrate, silver sulfadiazine and in combination with proteins. Actually, silver sulfadiazine works as a broad-spectrum antibiotic used mainly in the treatment of burn wounds. However, most of the current clinical silver agents all have their own disadvantages limiting their clinical usefulness.

Therefore, based on the benefits of silver, the pressing interest in finding new silver pharmaceuticals promoted the development of more efficient and convenient silver agents, in which employing ligands that can strongly coordinate to the active silver (I) ions is essential. [2f] In recent years, systematic discovery and development of silver complexes yielded a large number of promising antibacterial, antifungal and even anticancer compounds and several reviews on the topics have been reported. Recently, Lobana *et al*. have studied the *in vitro* antimicrobial potencial and biosafety evaluation of silver(I) derivatives of several thio-ligands, some of which have shown significant antimicrobial activity and low cellular toxicity with high percent cell viability. [9a-c] Hadjikakou *et al*. have reviewed the antiproliferative activity of silver (I) compounds [9d] in comparison with the corresponding one of cisplatin, a clinical chemotherapeutic drug currently in use. Liang *et al*. have also rencently reviewed the recent advances in the medical use of silver complexes. [2f] Other more general reviews concerning metallodrugs have also recently been reported. [5, 10] These surveys show that silver (I) complexes exhibit selectivity against a variety of cancer cells and bacterial strains in regard to the kind of ligands coordinated to silver (I) ions. However, the research in this field is still limited at present. Most studies focus on the Ag(I)-NHC complexes. [11] New ligands for better activity and lower toxicity need to be studied further. Besides, more research is still required to fully elucidate the mechanism of action of silver (I) complexes against both microorganism and tumor cells. [5]

Since its synthesis for the first time in 1834, hexachlorocyclotriphosphazene, [$N_3P_3Cl_6$], has been an important compound of phosphorus chemistry as a scaffold, and a large number of cyclotriphosphazene derivatives (CCPZ) and their analogue polymers, polyphosphazenes (PPZ), have been synthesized and applied in various fields such as biology, catalysis, fluorescence, nanomaterials, etc. [12] Today, one of the most important use concerns its biomedical applications. [13] Phosphazenes comprise a broad class of molecules based on the repeating unit [NPR_2] and include cyclic or linear oligomers and polymers. The most striking characteristic of this type of compound is its associated synthetic versatility, which enables the introduction of almost any substituent group R at phosphorous and allows properties to be taloired by the choice of appropriate functional groups. [12] Notably, biocompatibility and biodegradability can be regulated by the introduction of specific side groups, R. [14] The degradation rate can also be controlled by external stimuli, such as temperature, radiation, pH of the degradation medium and

degradation product solubility. [14] Nowadays, the use of PPZs in drug-delivery applications, especially proteins and anti-cancer drug-delivery, has become a significant focus. [13b, 15] The effects of various side groups on the properties of resultant PPZs and their use in different approaches, such as drug delivery, have recently been reviewed. [13b] Macromolecular pro-drugs are known to show excellent tumor targeting properties by the enhanced permeability and retention (EPR) effect [16] and exhibit improved body distribution and prolonged blood circulation, due to the dominant pharmacokinetic properties of macromolecular carrier. [17] In this respect, drugs can be physically encapsulated by liposomes, nanocapsules or polymeric micelles or vesicles and, alternatively, conjugated to linear polymer o dendrimers by covalent bonding. Drug-polymer conjugate is an emerging area of drug delivery in order combat the hurdles related to the delivery of drugs such as low solubility, protection against degradation by various factors, low bioavailability and high dose toxicity. Thus, some antibiotic, anti-viral, antitumoral or anti-malarial drugs have been conjugated to PPZ and CCPZs. [13] CCPZs are even in a much better position than PPZs, because the phosphazene trimer backbone is monodisperse and it is much easier to control the purity and molecular weight of these molecules, [13a] which both play a critical role for its clinical use. Besides, CCPZs can be used as core of dendrimers giving rise to a wide variety of branched molecules, which have a precise structure and are also monodisperses. [18] Over the last few years, cyclotriphosphazene has been developed in several pharmacological domains [19] and the use of dendrimers in general and dendrimers based on cyclotriphosphazene core in particular has been said to represent a new strategy in nanomedicine. Recent developments of CCPZ for major pharmaceutical applications have been reviewed by Majoral *et al*. [13c] Besides, both PPZs and CCPZs can be used as scaffolds for the design and construction of a variety of ligands, [12c, 20] to coordinate to metallic drugs. The facile substitution of P-Cl bonds in cyclic trimer, hexachlorocyclotriphosphazene [$N_3P_3Cl_6$], allows ready construction of cyclophosphazenes carrying additional exocyclic donor functions giving a library of multi-site coordination ligands. Furthermore, the ring nitrogen atoms have sufficient basicity to coordinate to metals depending on the electronic properties of the exocyclic substituents at phosphorus. Alkyl, aryl and primary and secondary organo amino substituents enhance the donor ability of N(ring) atoms. [20c]

Several authors have prepared and studied the tumoral properties of cyclo- or polyphosphazene-platinum(II) conjugates. [21] Recently, Henke *et al* introduced PPZ-

based anti-cancer prodrug conjugates in which cisplatin and oxaliplatin were first converted into prodrugs and then attached to the PPZ through a linker. [22] Silver derivatives of phosphazenes (cyclic or polymers) are also known. [23] The Steiner group has published interesting work using (amino)cyclophosphazenes to prepare structurally characterized silver(I) coordination polymers by formation of linear N-Ag-N connections via nitrogen centers of the phosphazene ring. [24]. We have also contributed to this field by reporting metallocyclo- and polyphosphazenes containing gold or silver and their thermolytic transformation into nanostructured materials or into metallic micro- and nanostructures deposited on silicon and silica surfaces. [25] PPZs and CPPZs decorated with Ag nanoparticles have also been synthesized. [26] However, to the best of our knowledge, there are no reports of silver-phosphazenes with biological properties, such as antimicrobial or antitumoral ones. Thus, the interesting biological properties of both silver(I) complexes and phosphazenes, discussed above, together with our experience in both the chemistry, of silver and phosphazenes, prompted us to prepare new silver-cyclotriphosphazenes and study their antimicrobial and antitumoral properties.

Herein, the reactivity of the multi-side (amino)cyclotriphosphazenes ligands, $[N_3P_3(NHCy)_6]$ and $[N_3P_3(NHCy)_3(NMe_2)_3]$, has been explored in order to obtain silver(I) metallophosphazenes complexes. For this purpose, the simple strategy used was to use silver(I) precursors bearing a phosphane ligand and a labile triflate (OTf) to be displaced by the phosphazene ligand. Thus, two series of silver(I) metallophosphazenes were obtained and studies of their anti-cancer activity in the human breast adenocarcinoma (MCF7) and human hepatocellular carcinoma (HepG2) cell lines were carried out. The antibacterial activity was also tested against the Gram-negative strains *Escherichia coli* and *Pseudomonas aeruginosa*, against the Gram-positive *Staphylococcus aureus* and against two *Mycobacterium tuberculosis complex* (MTBC) strains, *M. tuberculosis* H37Rv and *M. bovis* BCG Pasteur. Comparison with the corresponding antiproliferative and antimicrobial activity of cisplatin and silver (I) nitrate, respectively, was also performed.

2. Results and discussion

2.1. Synthesis and characterization of the starting cyclotriphosphazenes: Syntheses of the starting cyclotriphosphazenes are outlined in Scheme 1.

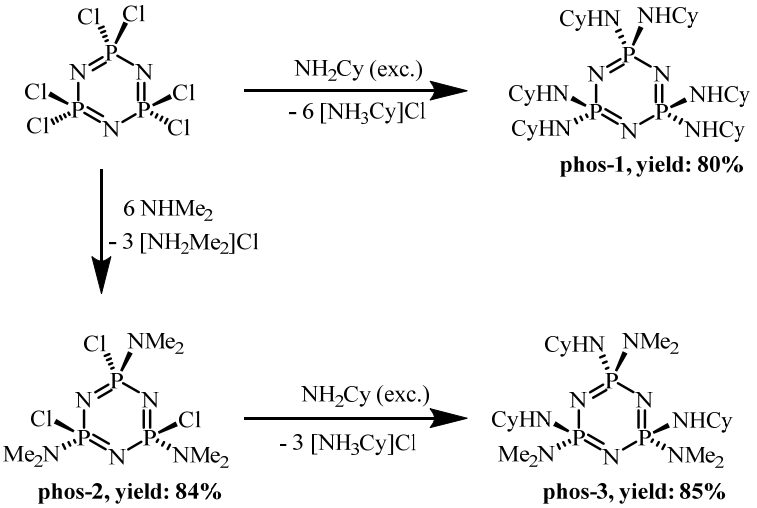

Scheme 1. Syntheses of the starting cyclotriphosphazenes

Specifically, the starting cyclotriphosphazenes, a single-substituent trimer, **phos-1**, and a mixed-substituent trimer, **phos-3**, were both prepared in high yield (>80%) from $[N_3P_3Cl_6]$ and *nongem-trans*-$[N_3P_3Cl_3(NMe_2)_3]$ **(phos-2)**, respectively, using tetrahydrofuran as a solvent and cyclohexylamine as a nucleophile and a base (see the Experimental Section). The synthesis of **phos-1** and **phos-2** has been described previously, [27-29] starting from hexachlorocyclotriphosphazene, $[N_3P_3Cl_6]$, but involving less efficient methods than those used by us. The trimer **phos-1** was prepared by Chandrasekhar *et al* using diazabicycloundecane (DBU) as a base and chloroform as a solvent [27, 28]. In this reaction the major product was the incompletely substituted derivative, $[N_3P_3Cl_2(NHCy)_4]$, and only prolonged reaction conditions (8 days heating under reflux) led to the fully single-substituted derivative, $[N_3P_3(NHCy)_6]$, which was formed only in minor yield (6.8%). [27] Compound **phos-2** was synthesized by Ford *et al*, using diethyl ether as a solvent at room temperature (yield 27%), and by Keat and Shaw at −78ºC (yield 49%). [29] Starting also from $[N_3P_3Cl_6]$ but using tetrahydrofuran as a solvent and with slow dropwise addition of dimethylamine as a nucleophile and a base at 0 ºC, we obtained **phos-2** in high yield (84%) (see the Experimental Section for details). The substitution reaction of $[N_3P_3Cl_6]$ has been extensively studied with primary interest in the regio- and stereochemical pathways. [30, 31] In particular, the partial substitution of hexachlorocyclotriphosphazene usually results not only in stoichiometrically different products but also in various geometrical and positional isomers that are not easy to separate. Thus, reactions leading to the trisubstituted material, $[N_3P_3Cl_3X_3]$, usually result not only in the formation of

trisubstituted regioisomers, i.e. 2,2,4- and 2,4,6- (numbering starts at the nitrogen atom), which are also referred to as geminal and nongeminal isomers respectively, but also di- and tetrasubstituted derivatives as minor products. Besides, the nongeminal materials can exist in two stereoisomeric forms, either with the three substituents on the same side of the mean plane of the phosphazene ring (nongeminal-*cis*-2,4,6) or with two on one side and the third on the other (nongeminal-*trans*-2,4,6) (see Chart 1).

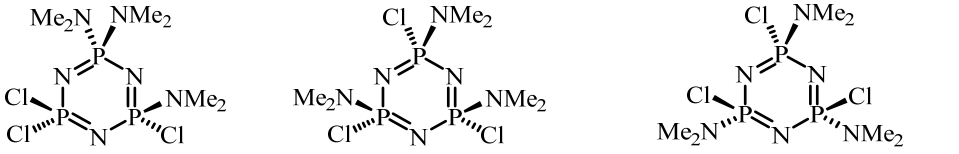

Chart 1. Trisubstituted cyclotriphosphazene isomers

As reported, some of variations in aminolysis patterns may be associated with experimental conditions, such as temperature, solvent and stoichiometry, which in some circumstances may determine the presence or absence of a particular isomer, or at least its relative proportions. [30] All three compounds we obtained, **phos-1** to **phos-3,** were completely characterized by elemental analysis, IR, ^{1}H, $^{13}C\{^{1}H\}$ and $^{31}P\{^{1}H\}$ NMR spectroscopy, and mass spectrometry. [32] All these data are given in the Experimental Section and are consistent with the formulae and structure indicated. Specifically, **phos-2** has a nongeminal-*trans* trisubstituted configuration. That nongeminal-*trans* configuration is maintained in the new phosphazene **phos-3** after the complete substitution of the chlorine atoms by cyclohexylamino units. Elemental and mass spectrometry analysis indicated that the compositions of **phos-2** and **phos-3** are $[N_3P_3Cl_3(NMe_2)_3]$ and $[N_3P_3(NHCy)_3(NMe_2)_3]$, respectively, and ^{1}H and $^{31}P\{^{1}H\}$ NMR spectroscopy analysis indicated that both have a nongeminal-*trans* configuration. NMR spectroscopy is one of the most powerful tools for the structural characterization of cyclophosphazenes, since the most critical structural information is available from the chemical shifts and spin-spin coupling data of their $^{31}P\{^{1}H\}$ NMR spectra. [30, 33, 34] Thus, the $^{31}P\{^{1}H\}$ NMR spectra of **phos-2** and **phos-3** showed a multiplet from a spin system AB_2, which indicates that both of them are nongeminal-*trans* (see Figure 1a for **phos-2** and Figure 2a for **phos-3**). The geminal trisubstituted derivative (I in chart 1) would have exhibited a spin system AX_2, i.e. a doublet and a triplet (both phosphorus would have

markedly different environments), and the nongeminal-cis trisubstituted derivative (II in chart 1) a spin system A_3, i.e. a singlet. The ^{1}H NMR spectra of all the dimethyl-aminolysis products of $[N_3P_3Cl_6]$ have been examined elsewhere, [29] as have those of the trisubstituted derivatives including *nongem-trans*-$[N_3P_3Cl_3(NMe_2)_3]$ **(phos-2)**. As the authors commented, [29] detailed interpretation of the ^{1}H NMR spectra is difficult because of their great complexity. At their simplest, when they contain only one type of dimethylamino environment, the spectrum consists of one doublet centered at approx. 2.50-2.70 ppm (with an additional broadened structure between the major peaks) [35] with a separation (apparent coupling constant, *J'*(P-H) or *N*) varying between 11 and 18 Hz. The *N* value is dependent on the nature of the second substituent bonded directly to the phosphorus carrying the $–NMe_2$ group. A $P(Cl)(NMe_2)$ group gives *N* of about 18 Hz and a $P(NMe_2)_2$ or $P(NR_2)(NMe_2)$ group gives about 11 Hz. [29] Thus, the coupling constants indicate the groups attached to the phosphorus atoms and the number of doublets indicate different sets of environments. The ^{1}H NMR spectrum of **phos-2** showed two pseudo-doublets, each with *N* approx. 18 Hz (see Figure 1b), as reported in the literature. [29a] This *N* value is in accord with the fact that the $–NMe_2$ groups are each located on a separate phosphorus atom (*nongeminal* derivative), i.e. $P(Cl)(NMe_2)$ groups . The presence of two pseudo-doublets confirms that **phos-2** is the *trans* isomer. The ^{1}H NMR spectrum of the new phosphazene **phos-3** is shown in Figure 2b, which presents the signals corresponding to the cyclohexylamino and dimethylamino units. For dimethyamino protons a multiplet centered at 2.62 ppm is observed with *N*= 13.6 Hz. As mentioned before, this *N* value is in accord with the presence of $P(NR_2)(NMe_2)$ groups.

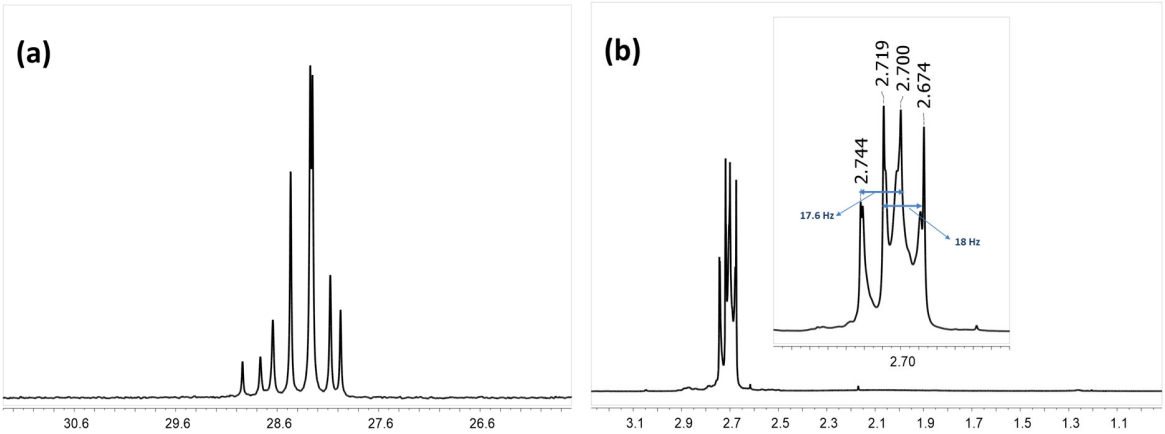

Figure 1. (a) $^{31}P\{^1H\}$ and **(b)** ^{1}H NMR spectra of compound **phos-2** in $CDCl_3$ (400 MHz)

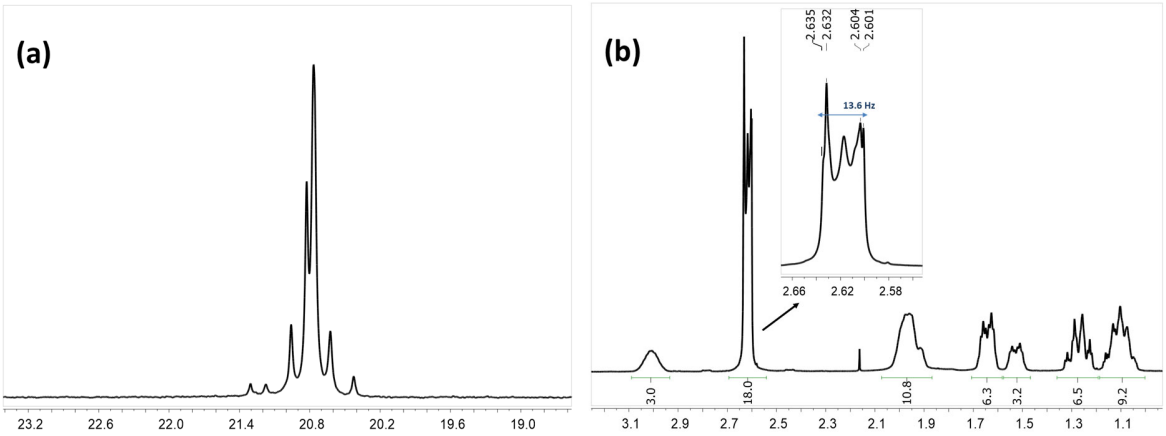

Figure 2. (a) $^{31}P\{^{1}H\}$ and **(b)** ^{1}H NMR spectra of compound **phos-3** in $CDCl_3$(400 MHz)

2.2. Synthesis and characterization of the metallophosphazenes: The reaction of **phos-1** or **phos-3** with the silver complexes [Ag(OTf)L] (L= PPh_3, PPh_2Me or TPA) (TPA= 1,3,5-triaza-7-phosphaadamantane) (OTf= OSO_2CF_3), in dichloromethane and in different molar ratios 1:2 or 1:3, led to two series of the cationic metallophosphazenes $[N_3P_3(NHCy)_6\{AgL\}_n](TfO)_n$ (n=2, L= PPh_3 (**2**), PPh_2Me(**4**); n=3, L= PPh_3 (**3**), PPh_2Me(**5**), TPA(**6**)) and *nongem-trans*-$[N_3P_3(NHCy)_3(NMe_2)_3\{AgL\}_n](TfO)_n$ (n=2, L= PPh_3 (**7**), PPh_2Me(**9**); n=3, L= PPh_3 (**8**), PPh_2Me(**10**)). In all of them the silver groups "AgL" are coordinated to the nitrogen atoms of the phosphazene ring, whereby their number (two or three) depends on the molar ratio used (see Scheme 2). The reaction of **phos-1** with the same starting complexes, [Ag(OTf)L] (L= PPh_3 or PPh_2Me), but in molar ratio 1:1, evolved in a more complex way, giving a mixture of compounds in which the major product was $[N_3P_3(NHCy)_6Ag(TfO)]_n$ (**1**). The identification of this derivative **1** was confirmed by the reaction of **phos-1** with AgTfO in molar ratio 1:1 (see Experimental Section).

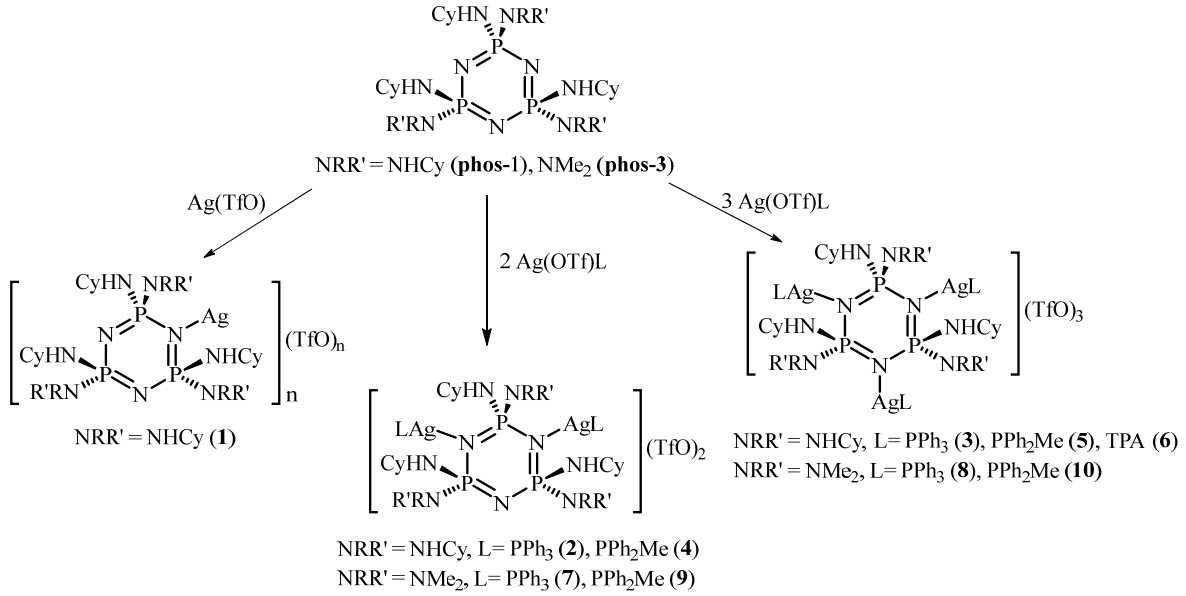

Scheme 2. Synthesis of new metallophosphazenes

All new metallophosphazenes **2-10** were obtained in high yield and could be handled and stored light protected under ambient conditions during large periods of time. They are soluble in dichloromethane, acetone, chloroform and DMSO and only slightly soluble or insoluble in hexane or pentane. Their solutions must also be handled and stored light protected and they were stable during at least a week at room temperature in these conditions, as was proved by $^{31}P\{^{1}H\}$ and ^{1}H spectroscopy. All of them are insoluble in water, even compound **6** bearing the water-soluble phosphane ligand 1,3,5-triaza-7-phosphaadamantane (TPA), which was prepared in an unsuccessful attempt to obtain a water-soluble metallophosphazene. Compound **1** is only sparingly soluble in dichloromethane, chloroform or acetone and insoluble in water, diethyl ether, ethanol, hexane or pentane. All these compounds **1-10** were characterized by elemental analysis, IR, ^{1}H, $^{13}C\{^{1}H\}$ and $^{31}P\{^{1}H\}$ NMR spectroscopy, and mass spectrometry. All these data are given in the Experimental Section and are consistent with the formulas and structure indicated and, specifically, with the coordination of metals to the backbone nitrogen atoms. In addition, X-ray structural analyses of **5**, **7** and **9** confirmed the proposed structures.

IR spectra of all of these complexes clearly evidence the coordination of the metal fragments, AgL, to **phos-1** or **phos-3**. Thus, the IR spectra show absorptions attributable to trifluoromethanesulfonate (triflate) units and to the phosphane ligands, which are all shifted from those in the starting complexes [Ag(OTf)L] (L= PPh_3, PPh_2Me or TPA). The triflate peaks, which could in principle be used to distinguish covalent and ionic

trifluoromethanesulfonate, [36] are not very useful because an unambiguous assignment is hindered by the overlap of CF_3, SO_3 and phosphane vibrational modes. [37] However, all **1**-**10** complexes have very similar bands in shape and position in the stretching region of the triflate (1280-1000 cm^{-1}, $\nu[SO_3(E)]$, $\nu[SO_3(A_1)]$, ν $[CF_3(A_1)]$ and ν $[CF_3(E)]$) (see Experimental Section). This is consistent with the presence of ionic trifluoromethanesulfonate, which was clearly confirmed in **7** and **9** by X-ray structural analyses. Besides, a single peak at approx. −78 ppm appears in the ^{19}F NMR spectra of all synthesized complexes. The bands of the characteristic phosphazene absorptions in the IR spectra, such as P=N and C-N (at 1186 and 1177 cm^{-1} in **phos-1** and 1180, 1171 and 1140 cm^{-1} in **phos-3**) change after coordination of the metal, as previously observed in other metallophosphazenes with silver coordinated to the backbone nitrogen atoms. [23c] However, new bands corresponding to these peak frequencies could not be assigned because of overlap with CF_3, SO_3 and phosphane vibrational modes. The bands in the 3000-3400 cm^{-1} region, which are assigned to the N-H stretching, are also different from those of the starting phosphazenes. On complexation, only one band at approx. 3300 cm^{-1} is observed for all complexes.

The $^{31}P\{^1H\}$ and ^1H NMR spectra in solution are also consistent with the coordination of the metal fragments to the ring nitrogen atoms. The signals observed for **2**-**6**, with the single-substituent trimer **phos-1**, in their $^{31}P\{^1H\}$ NMR spectra at room temperature (RT), are collected in Table 1. A single peak, shifted downfield from the peak of the parent phosphazene, is shown by the phosphazene phosphorus atoms in all complexes **2**-**6**. This downfield shift can be ascribed to deshielding by the silver ion coordinated to the adjacent nitrogens, which increases with the number of metals linked to adjacent nitrogens. This shift has also been observed in other metallophosphazenes in which metals (such as silver or lithium) are coordinated to the backbone nitrogen atoms. [23b, 23c] The signal observed at RT is a single peak even for **2** and **4,** for which a AX_2 spin system corresponding to two types of phosphorus atoms would be expected. This is attributable to a fluxional process, which is typical in the coordination chemistry of silver and can be attributed to exchange phenomena involving all the phosphazene nitrogen atoms. Fluxionality can be quenched at low temperature. Thus, the single broad peak observed for the phosphazene phosphorus atoms in **2** and **4** at RT is split into two signals at −80ºC (as shown in Figure 3 for **4**; see also Table 2). The sparingly soluble compound **1**,

$[N_3P_3(NHCy)_6Ag(TfO)]_n$, was not fluxional in solution, and two signals were observed for the phosphazene phosphorus atoms in its $^{31}P\{^1H\}$ NMR spectrum at RT (10.39 ("t, 1P) and 8.43 ("d", 2P), AB_2 system $^2J_{AB}$ = 45.1 Hz). Both the poor solubility and the non-fluxionality might be associated with the oligomeric or polymeric nature of **1**. However, single crystals suitable for X-ray diffraction analysis could not be obtained.

Table 1. $^{31}P\{^1H\}$ NMR Spectroscopic Data for **2-6** and starting products.[a]

COMPOUND	δ[N-*P*-N]	δ[*P*R$_3$] [^{1}J(^{109}Ag-P)][b], [^{1}J(^{107}Ag-P)][b]
$[N_3P_3(NHCy)_6]$ **(phos-1)**	14.44(s)	—
$[Ag(OTf)PPh_3]$	—	16.79 (br)
$[N_3P_3(NHCy)_6\{AgPPh_3\}_2](TfO)_2$ (**2**)	16.90 (br)	17.12 (dd) [746.1], [653.4]
$[N_3P_3(NHCy)_6\{AgPPh_3\}_3](TfO)_3$ (**3**)	18.38 (s)	16.53 (dd) [761.7], [662]
$[Ag(OTf)PPh_2Me]$	—	−3.13 (br)
$[N_3P_3(NHCy)_6\{AgPPh_2Me\}_2](TfO)_2$ (**4**)	16.22 (br)	−1.90 (dd) [757.6], [651.4]
$[N_3P_3(NHCy)_6\{AgPPh_2Me\}_3](TfO)_3$ (**5**)	18.57 (s)	−2.78 (d,br) [718]
[Ag(OTf)TPA]	—	−85.82 (br)
$[N_3P_3(NHCy)_6\{AgTPA\}_3](TfO)_3$ (**6**)	15.93(s)	−85.46 (br)

[a] Data taken at room temperature in $CDCl_3$, except for **6** and [Ag(OTf)TPA], whose data are in DMSO. Values in ppm. [b] Values in Hz.

Table 2. $^{31}P\{^1H\}$ NMR Spectroscopic Data for **2** and **4** at room temperature and at -80ºC.

COMPOUND	Spin system	T	δ[N-*P*-NAg] [a] [^{2}J(P-P)] [b]	δ[AgN-*P*-NAg] [a]	δ[*P*R$_3$] [a] [^{1}J(^{109}Ag-P)] [b], [^{1}J(^{107}Ag-P)] [b]
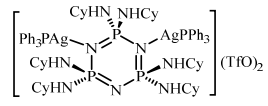 (**2**)	AX_2	RT	16.11 (br)		17.48 (dd) [748.9], [652.6]
		-80ºC	13,23 (d) [36.3]	17.54 (t)	17.51 (dd) [740.6], [641.3]
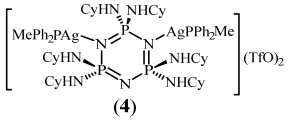 (**4**)	AX_2	RT	16.24 (br)		−1.25 (dd) [757.8], [653.5]
		-80ºC	13.50 (d) [36.9]	17.20 (t)	0.64 (dd) [753.9], [652.4]

[a] Data taken in $(CD_3)_2CO$. Values in ppm. [b] Values in Hz.

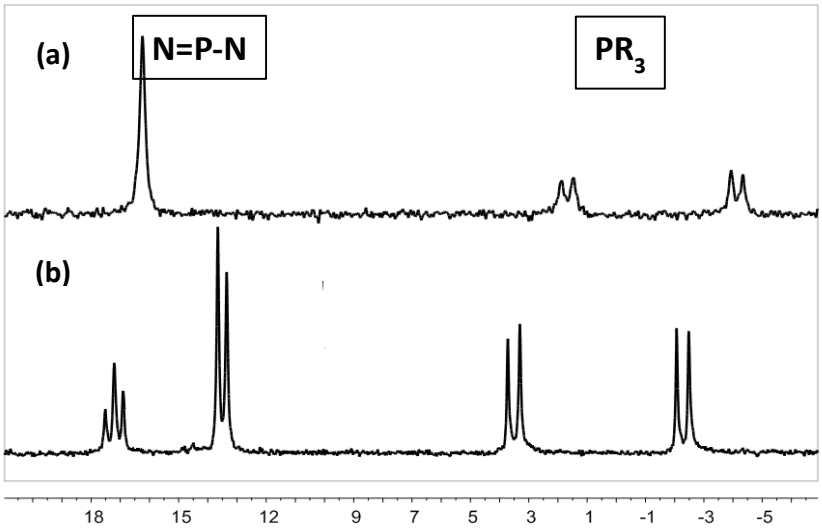

Figure 3. $^{31}P\{^{1}H\}$ NMR spectra of compound **4** in $(CD_3)_2CO$ (400 MHz) **(a)** at room temperature and **(b)** at −80ºC

The $^{31}P\{^{1}H\}$ NMR spectra of **2-6** also show the signals from the phosphane ligands (see Tables 1 and 2), which are all shifted from those in the starting complexes. [37, 38] For **6**, the phosphane resonates at −85.46 (s) ppm, which is consistent with a silver (I) compound containing TPA acting as a P-donor ligand. [39] Unlike **2**-**5**, this signal for **6** consists of a broad singlet at RT, the coupling with the two silver isotopomers (^{107}Ag and ^{109}Ag) is not observed, which indicates that the fluxional process in this compound also involves the TPA ligand. The ^{1}H NMR spectra of **2**-**6** (see Experimental Section) also show the signals corresponding to the phosphane ligands and the signals from the cyclohexylamino units (Table 3). These signals, specifically those of N*H* and NH-C*H*, were verified by two-dimensional heteronuclear (HSQC ^{1}H-^{13}C) correlations. Most significantly, the ^{1}H NMR spectra of **2**-**6** all show a unique type of cyclohexylamino units at RT, as a result of the above-mentioned fluxional process. For **2** and **4**, though, two types of NHCy units were observed when the spectra were collected at −80ºC, as a consequence of the non-equivalence of all the amino units. Thus, the single broad peak corresponding to the N*H* protons, which was observed at 4.03 (br, 6H) and 4.0 (br, 6H) ppm for **2** and **4** respectively in $(CD_3)_2CO$ at RT, was split into two signals at −80ºC (4.65 (t, 2H) and 4.40 (br, 4H) for **2**; 4.55 (br, 2H) and 4.20 (br, 4H) for **4**) (see Experimental Section). As can be observed in Table 3, which presents the ^{1}H NMR data in $CDCl_3$ at RT, coordination at phosphazene

leads in all complexes to a deshielding of the protons N*H*, with the rise in the number of metals coordinated to adjacent nitrogens.

Table 3. ^{1}H NMR Spectroscopic Data for **phos-1** and complexes **2-6.** *[a]*

COMPOUND	*δ*[N*H*]	*δ*[NH-C*H*]	*δ*[NH(C_6H_{11})]	*δ*[PPR_3]
$[N_3P_3(NHCy)_6]$ **(phos-1)**	2.0 (br,6H)	3.05 (m,6H)	1.94, 1.65, 1.50, 1.26, 1.10 (m, 60 H)	–
$[N_3P_3(NHCy)_6\{AgPPh_3\}_2](TfO)_2$ (**2**)	3.20 (br,6H)	3.0 (br,6H)	1.90, 1.87, 1.66, 1.54, 1.40,1.26-1.07(m,60H)	7.54-7.40 (m, 30H; *Ph*)
$[N_3P_3(NHCy)_6\{AgPPh_3\}_3](TfO)_3$ (**3**)	4.20 (br,6H)	3.02 (br,6H)	1.86, 1.46, 1.34, 1.25, 1.04-0.85 (m, 60H)	7.49-7.42 (m, 45 H; *Ph*)
$[N_3P_3(NHCy)_6\{AgPPh_2Me\}_2](TfO)_2$ (**4**)	3.5 (br,6H)	2.95 (br,6H)	1.85, 1.59, 1.42, 1.21, 1.06 (m, 60H)	7.60-7.41(m, 20H; *Ph*) 2.11(d, 6H, $^{2}J_{P-H}$= 5.9Hz; *Me*)
$[N_3P_3(NHCy)_6\{AgPPh_2Me\}_3](TfO)_3$ (**5**)	4.27 (br,6H)	2.96 (br,6H)	1.85, 1.50, 1.39, 1.24, 1.06-0.88 (m, 60H)	7.58-7.44(m, 30H; *Ph*) 2.11(d, 9H, $^{2}J_{P-H}$= 7.6Hz; *Me*)
$[N_3P_3(NHCy)_6\{AgTPA\}_3](TfO)_3$ (**6**)	3.41 (br,6H)	2.86 (br,6H)	1.85, 1.65, 1.53, 1.15 (m, 60H)	4.59 ("d"), 4,42 ("d") (AB system, 18H, $^{2}J_{H-H}$= 12.6 Hz; NCH_2N), 4.24 (br, 18H; PCH_2N)

[a] Data taken at room temperature in $CDCl_3$, except for **6**, whose data are in DMSO. Values in ppm.

The signals for the phosphazene phosphorus atoms for **7-10** also shift downfield relative to the parent phosphazene in their $^{31}P\{^{1}H\}$ NMR spectra at RT (See Table 4). However, even in **8** and **10** (both with three silvers), several signals are observed because of the nongeminal-*trans* configuration of the starting phosphazene **phos-3**, which is expected to be maintained in all metallophosphazenes **7**-**10**. Thus, the part of the spectrum corresponding to the phosphazene phosphorus in the $^{31}P\{^{1}H\}$ NMR spectra at RT show a single set of resonances of an AB_2 spin system for **10**, with peak centered at δ = 24.07 ("d", 2P) and 23.08 ("t", 1P), $^{2}J_{(P-P)}$= 33.1Hz, and a broad signal at 24.27 ppm for **8**. For **7** and **9**, this part of the spectrum (between 24-19 ppm) is even more complex, as is shown in Figure 4b for **9** as an example, with signals that are broad as a consequence of the above-mentioned fluxional process. In these compounds **7** and **9**, two diastereomers **A**

and **B** are expected (see Chart 2), namely, a pair of R_{P2},R_{P3}- or S_{P2},S_{P3}-configured enantiomers (**B**) and the diastereomer R_{P1},R_{P2},S_{P3} (**A**). At -80 ºC, two sets of resonances of two AB_2 spin systems are observed for **9** in this part of the spectrum when the fluxional process is quenched (see Figure 4a), which indicates that both stereoisomers **A** and **B** are present in solution. [40] The part of the spectrum corresponding to the phosphane ligands (see also Figure 4a) shows two set of two doublets, consistent with the presence of both diastereomers. [41]

Table 4. $^{31}P\{^1H\}$ NMR Spectroscopic Data for **7-10** and starting products. *[a]*

COMPOUND	δ[N-*P*-N] *[a]* [^{2}J(P-P)] *[b]*	δ[*P*R$_3$] *[a]* [^{1}J(^{109}Ag-P)] *[b]*, [^{1}J(^{107}Ag-P)] *[b]*
$[N_3P_3(NHCy)_3(NMe_2)_3]$ (**phos-3**)	20.96; 20.70 [44.3]	—
$[Ag(OTf)PPh_3]$	—	16.79 (br)
$[N_3P_3(NHCy)_3(NMe_2)_3\{AgPPh_3\}_2](TfO)_2$ (**7**)	24.20 (“d”, 2P), 23.0 (“t”, 1P) [36.2]	16.58 (dm) [671.5]
$[N_3P_3(NHCy)_3(NMe_2)_3\{AgPPh_3\}_3](TfO)_3$ (**8**)	24.27 (br)	16.19 (br)
$[Ag(OTf)PPh_2Me]$	—	−3.13 (br)
$[N_3P_3(NHCy)_3(NMe_2)_3\{AgPPh_2Me\}_2](TfO)_2$ (**9**)	23.55 (dbr, 2P), 21.05(tbr, 1P) [40]	−2.13 (dd) [765.0], [665.2]
$[N_3P_3(NHCy)_3(NMe_2)_3\{AgPPh_2Me\}_3](TfO)_3$ (**10**)	24.07 (“d”, 2P), 23.08 (“t”, 1P) [33.1]	− 3.10 (br)

[a] Data taken at room temperature in $CDCl_3$. Values in ppm. *[b]* Values in Hz.

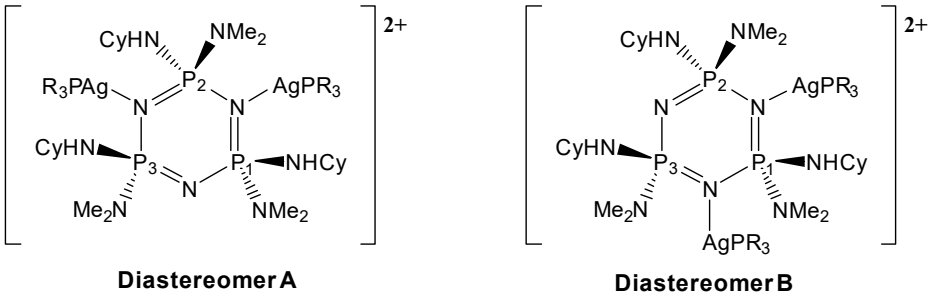

Diastereomer A **Diastereomer B**

Chart 2. Diastereomers expected for compounds **7** and **9**

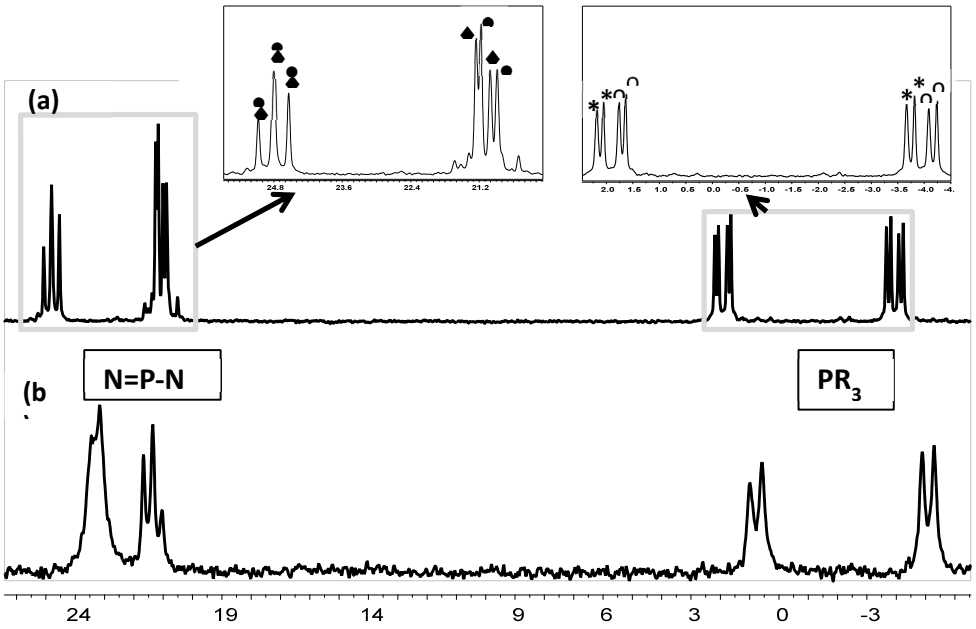

Figure 4. $^{31}P\{^{1}H\}$ NMR spectra of compound **9** in CD_2Cl_2 (400 MHz) **(a)** at −80ºC and **(b)** at room temperature

In the ^{1}H NMR spectra of **7**-**10**, the NH-C*H* protons resonate as a single broad signal at approx. 2.9 ppm and the N*H* protons resonate as two broad signals even at RT, as a result of the non-equivalence of all the amino groups due to the nongeminal-*trans* configuration of the phosphazene ring. The N*H* protons are also shielded upon coordination. All these data are collected in the Experimental Section, as are the $^{13}C\{^{1}H\}$ NMR, mass spectral and microanalytical data. It is worth noting that the molecular cations of almost all complexes **2-10** are observed in the mass spectra.

The single-crystal X-ray analyses of the racemic complexes **7** and **9** show that in both cases the R_{P2},R_{P3}- (and S_{P2},S_{P3}-) configured diastereomer is present (see Figures 6 and 7). Single crystals of **5**, **7.**$2CH_2Cl_2$ and **9.**$1/2\ C_6H_{14}$ were grown by slow diffusion of hexane into a solution of the complex in dichloromethane. The X-ray analysis confirmed not only the presence of ionic trifluoromethanesulfonate, but also the coordination of metals to the ring nitrogen atoms (see Figures 5-7). In the case of **5**, the structure was only confirmed qualitatively, but could not be refined satisfactorily because of severely disordered anions and unidentified solvent regions. Selected bond lengths and angles, and details of the data collection and refinement for **7** and **9** are given in Tables in the Supporting Information. In both compounds **7** and **9**, the silver atoms show a nearly linear coordination

with angles close to 180 º (167.97(8) and 165.57(8)° for **7**; 168.26(4) and 177.26(4)° for **9**). The Ag-N and Ag-P bond lengths are typical. [23g, 24a, 37a, 42] There are also short Ag…O contacts: for **7**, Ag2…O1 2.704(4) and for **9**, Ag1…O1 2.781(2) and Ag2…O5 2.870(3) Å. Metalation causes distortion of the cyclophosphazene ring skeleton. The P-N(ring) bonds associated with metal coordination are longer (av. 1.627(3) Å for **7** and 1.6270(15) Å for **9**) than the P-N(ring) bonds at the noncoordinating N center (av. 1.583(3) Å for **7** and 1.5861(15) Å for **9**) and also the P-N(ring) bonds in the starting phosphazene [$N_3P_3(NHCy)_6$] (**phos-1**) (1.598 Å). [28, 43] Such an N-P bond-length increase flanking the site of coordination (or protonation or alkylation) is known from studies on cyclotriphosphazenes. [23g, 24a, 44, 45] This is consistent with bonding model of Graig and Paddock. [46] Accordingly, in such situations the lone pair on the ring nitrogen of the cyclophosphazenes is not available for π-bonding interactions within the ring, causing an increase in the affected bond distance. The exocyclic P-N bond lengths (av. 1.632(3) for P-NHCy and 1.649(3) for P-NMe_2 in **7**; 1.6341(16) for P-NHCy and 1.6530(16) for P-NMe_2 in **9**) are longer than the P-N(ring) bond lengths but are shorter than the ideal P-N single-bond value of 1.77 Å. [27, 30c] While the phosphazene rings of the free ligands, i.e. **phos-1**, are planar or close to planarity, [43] the coordination to silver causes the rings to pucker, which is evident from the ring torsion angles (maximum absolute values of 24.5(3)º in **7** and 32.9(1)º in **9)**.

The NH groups of the ligands form classical hydrogen bonds to the triflate anions: for **7**, N4…O1 2.964(4), N6…O4 2.968(4) and N8…O2 3.135(5) Å and for **9**, N4…O4 2.991(3), N6…O2 3.020(2) and N8…O4 3.374(3) Å.

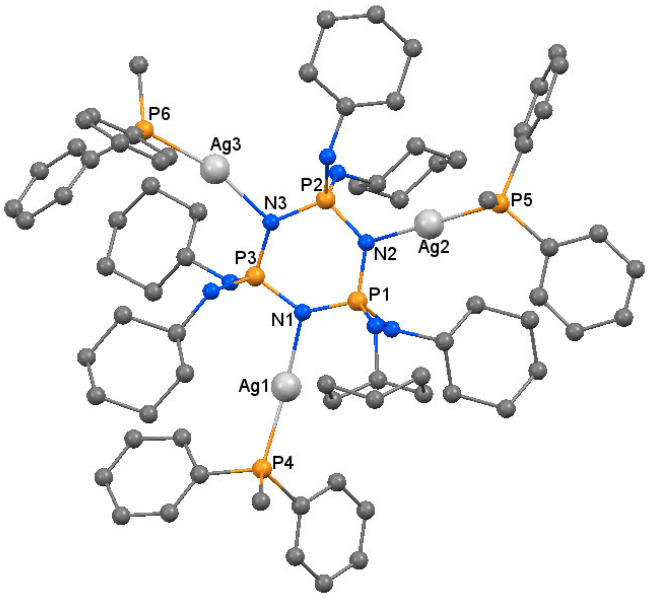

Figure 5. Molecular structure of complex **5** determined by single-crystal X-ray diffraction. Hydrogen atoms, anions and solvent molecules have been omitted for clarity. Radii are arbitrary.

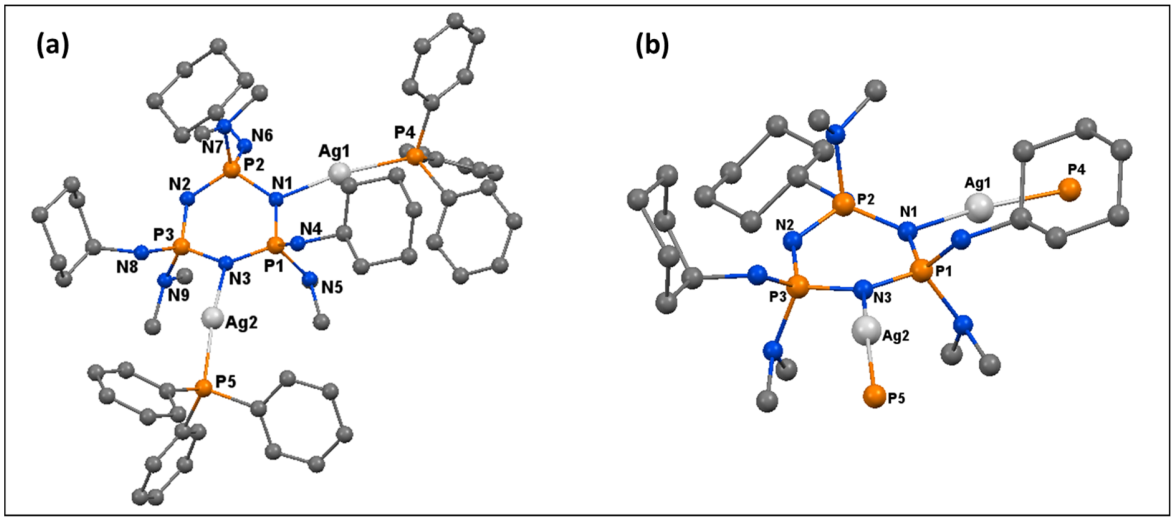

Figure 6. Molecular structure of complex **7** determined by single-crystal X-ray diffraction. Hydrogen atoms, anions and solvent molecules have been omitted for clarity. Radii are arbitrary.

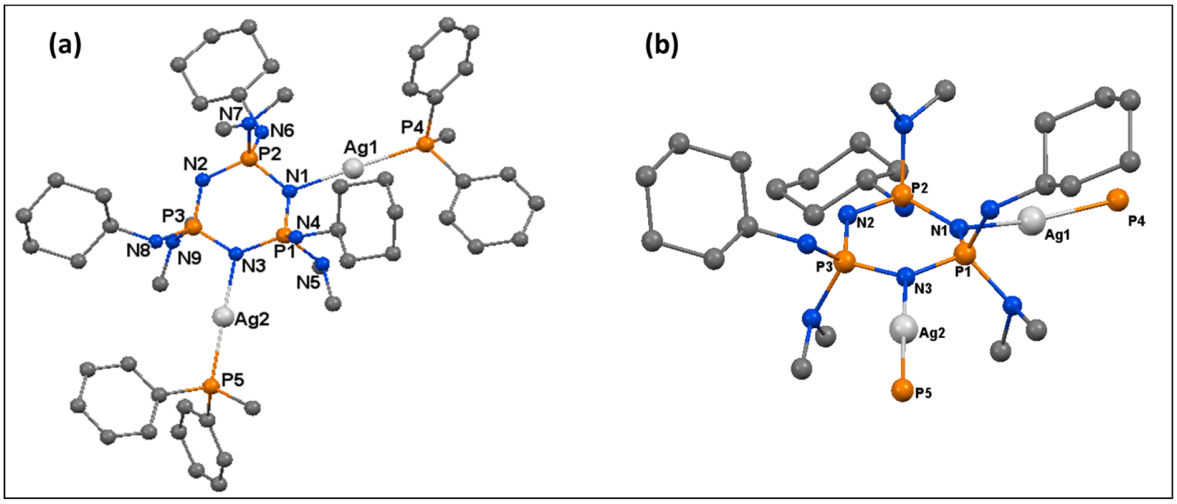

Figure 7. Molecular structure of complex **9** determined by single-crystal X-ray diffraction. Hydrogen atoms, anions and solvent molecules have been omitted for clarity. Radii are arbitrary.

2.3. Biological Evaluation: Cytotoxic and antibacterial activity

All the complexes are insoluble in water but are soluble in DMSO and in the DMSO/water mixtures used in the biological tests (cytotoxic and antibacterial ones). In the cytotoxicity tests, the mixtures used contain a minimal amount of DMSO (≤ 0.1%). In the antibacterial tests, the solvent DMSO was also used as a control (in the same percentage used to dissolve the compounds) so as to confirm that it did not inhibit bacterial growth. While performing the tests, no precipitation of any compound at the concentration ranges assayed was observed. The colourless DMSO solutions were very stable at room temperature. The stability of compounds in DMSO was provided by ^{31}P and ^{1}H NMR spectroscopy. As supplementary material, we have included these spectra for compound **2**, as an example, measured over 48 hours, which is the time for the biological assays. These spectra showed the expected signals according to the proposed structure for compound **2**, slightly displaced with respect to those observed for the same complex in other solvents such as acetone, which remain exactly the same in more than 48 hours. Among the new metallophosphazenes **1**-**10**, we have selected **2**-**6**, **9** and **10** to carry out the biological studies so as to evaluate the structure-activity relationship. Under the same conditions, cisplatin and silver (I) nitrate, two well-known chemotherapeutic and antimicrobial drugs respectively, have been tested and compared to all the compounds studied.

Cytotoxic activity

The *in vitro* cytotoxicity of the new complexes **2-6**, **9** and **10** and their precursors (the phosphazene ligands -**phos1** and **phos3**- and the silver starting complexes) has been evaluated against two tumour human cell lines, MCF7 and HepG2, by two different biomarkers, Alamar Blue (AB) and Neutral Red Uptake (NRU) after 48h of exposure. At 24h the exposed cells were checked under the optical microscope and the damage was observed at the similar range which has been calculated after 48h (See Supplementary Material). By using both viability assays, median inhibitory concentration (IC_{50}) values (Table 5 a,b) were calculated from the dose-response curves obtained by non-linear regression analysis. IC_{50} values are concentrations of a drug required to inhibit tumour cell proliferation by 50% compared to non-treated cells.

Table 5. IC_{50} obtained by Alamar Blue and Neutral Red Uptake in MCF7 (a) and HepG2 (b) cell lines exposed to the new metallophosphazenes and their precursors after 48 h.[a]

	Compound	IC_{50} (μM)	
		Alamar Blue	**Neutral Red Uptake**
MCF7(a)	$N_3P_3(NHCy)_6$ **(phos-1)**	14.80 ± 6.10	>25
	$[N_3P_3(NHCy)_6\{Ag(PPh_3)\}_2](TfO)_2$ (**2**)	2.87 ± 0.15	2.34 ± 0.28
	$[N_3P_3(NHCy)_6\{Ag(PPh_3)\}_3](TfO)_3$ (**3**)	1.60 ± 0.05	2.14 ± 0.65
	$[Ag(OTf)PPh_3]$	5.67 ± 0.57	8.09 ± 1.39
	$[N_3P_3(NHCy)_6\{Ag(PPh_2Me)\}_2](TfO)_2$ (**4**)	4.89 ± 1.08	2.45 ± 0.66
	$[N_3P_3(NHCy)_6\{Ag(PPh_2Me)\}_3](TfO)_3$ (**5**)	3.88 ± 0.11	3.64 ± 0.05
	$[Ag(OTf)PPh_2Me]$	11.76 ± 2.88	14.02 ± 1.05
	$[N_3P_3(NHCy)_6\{Ag(TPA)\}_3](TfO)_3$ (**6**)	4.46 ± 0.01	3.32 ± 0.12
	[Ag(OTf)TPA]	59.93 ± 11.36	30.74 ± 3.06
	$N_3P_3(NMe_2)_3(NHCy)_3$ **(phos-3)**	16.58 ± 4.76	7.81 ± 0.02
	$[N_3P_3(NMe_2)_3(NHCy)_3\{Ag(PPh_2Me)\}_2](TfO)_2$ (**9**)	5.48 ± 0.18	5.95 ± 0.49
	$[N_3P_3(NMe_2)_3(NHCy)_3\{Ag(PPh_2Me)\}_3](TfO)_3$ (**10**)	4.18 ± 0.18	3.44 ± 0.10
	Cisplatin	56.82 ± 4.23	23.71 ± 1.24

	Compound	IC_{50} (μM)	
		Alamar Blue	**Neutral Red Uptake**
HepG2 (b)	$N_3P_3(NHCy)_6$ **(phos-1)**	>25	>25

	$[N_3P_3(NHCy)_6\{Ag(PPh_3)\}_2](TfO)_2$ (**2**)	1.40 ± 0.23	2.41 ± 0.18
	$[N_3P_3(NHCy)_6\{Ag(PPh_3)\}_3](TfO)_3$ (**3**)	0.93 ± 0.37	1.37 ± 0.55
	$[Ag(OTf)PPh_3]$	4.45 ± 0.37	7.69 ± 1.96
	$[N_3P_3(NHCy)_6\{Ag(PPh_2Me)\}_2](TfO)_2$ (**4**)	2.38 ± 0.12	2.61 ±0.43
	$[N_3P_3(NHCy)_6\{Ag(PPh_2Me)\}_3](TfO)_3$ (**5**)	2.16 ± 0.13	2.63 ±0.39
	$[Ag(OTf)PPh_2Me]$	11.02 ± 0.09	14.03 ± 1.04
	$[N_3P_3(NHCy)_6\{Ag(TPA)\}_3](TfO)_3$ (**6**)	2.02 ± 0.34	5.48 ± 0.23
	[Ag(OTf)TPA]	45.88 ± 3.34	29.31 ± 4.09
	$N_3P_3(NMe_2)_3(NHCy)_3$ **(phos-3)**	8.80 ± 0.69	10.25 ± 2.05
	$[N_3P_3(NMe_2)_3(NHCy)_3\{Ag(PPh_2Me)\}_2](TfO)_2$ (**9**)	2.82 ± 0.20	4.05 ± 0.24
	$[N_3P_3(NMe_2)_3(NHCy)_3\{Ag(PPh_2Me)\}_3](TfO)_3$ (**10**)	2.76 ± 0.22	3.20 ± 0.24
	Cisplatin	11.32 ± 1.11	6.94 ± 0.72

[a] All the compounds analysed were dissolved in DMSO, not exceeding 0.1%, except cisplatin, which was dissolved in water.

All the tested metallophosphazenes, **2-6, 9** and **10**, showed excellent antitumour activities towards MCF7 cell line with IC_{50} values lower than 5,5 μM (see Table 5a), the best of these were complexes **2** and **3** with IC_{50} values with both biomarkers lower than 3 μM. Except [Ag(OTf)TPA], all the compounds we tested were more cytotoxic than cisplatin towards MCF7. Besides, all the new metallophosphazenes (**2-6, 9** and **10**) were more cytotoxic than their phosphazene ligands and silver precursors and much more cytotoxic than cisplatin, which showed IC_{50} values of 56.82 and 23.71 μM in the AB and NRU assays, respectively. In general, NRU proved to be a more sensitive assay for MCF7 cells than AB except for compound **3**, in which both of them are similar.

The cytotoxicity of all metallophosphazenes acquired in HepG2 cells was even more drastic than in MCF7 (Table 5b). In the AB assay, the obtained IC_{50} values were lower than 3 μM, also being **2** and **3** the most cytotoxic compounds, with values of 1.40 and 0.93 μM, respectively. In this case, in contrast to the results we found for MCF7, the biomarker AB was more sensitive in comparison to NRU. Once more, all metallophosphazenes showed lower IC_{50} values than their precursors and cisplatin, with values of 11.32 and 6.94 μM in the AB and NRU assays, respectively, being the new silver phosphazenes extraordinarily effective as cytotoxic agents *in vitro*. Regarding the cytotoxicity of the

precursors in HepG2 cells, only [Ag(OTf)PPh_3] was just as or even more cytotoxic than cisplatin but also much less cytotoxic than their silver phosphazenes, **2** and **3**.

As for the structure-activity relationships towards both cell lines in these metallophosphazenes **2-6, 9** and **10**, the following can be concluded: (1) the silver atom exerts the cytotoxic activity, which is significantly enhanced by the rise in the number of silvers linked to the phosphazene ring (see Table 5a,b; **3** is more toxic than **2**, **5** more than **4** and **10** more than **9)**; (2) the ligands coordinated to silver also have an influence in the cytotoxicity, which is higher in triphenylphosphane derivatives than in those with diphenylmethylphosphane or TPA (see Table 5a,b; **3** is more toxic than **5** or **6**). Moreover, the cytotoxicity was also higher in those with the phosphazene ligand **phos-1** than those with **phos-3** (see Table 5a,b; **4** is more toxic than **9** and **5** more than **10**). Thus, **3** is the most toxic compound, followed by **2**. Remarkably, both metallophosphazenes **2** and **3** were just as toxic as auranofin, a well-known cytotoxic gold(I) compound which is even more toxic than cisplatin for MCF7 and HepG2 cells. IC_{50} values reported for auranofin are 1.1 μM for MCF7 cells [47] and 2.0 μM para HepG2 [48]. The anticancer activity of silver(I) complexes has been summarized in recent reviews [2f, 9, 11c] and the IC_{50} values obtained for all the tested silver phosphazenes are among the lowest found for any silver derivatives against MCF7 and HepG2 cell lines, taking into account the experimental conditions (measured at 48 h). To the best of our knowledge, the lowest IC_{50} values found in the literature for silver complexes against the mentioned cell lines have been described by Hadjikakou *et al*. (IC_{50} range between 1.6 to 2.5 μM in MCF7, for acetylsalicylate or hydroxybenzoic acid derivatives), [49] by Galal *et al*. (IC_{50} value of 2.0 μM in MCF7, for a complex of 2-methyl-1H-benzimidazole-5-carboxylic acid hydrazide), [50] by Gautier [51], Hague [52] or Tacke [53] (IC_{50} value < 0.4 μM, 0.9 μM or ranging from 1.4-5.8 μM in MCF7, respectively, all of them for carbene complexes), by Yilmaz *et al*. (IC_{50} ranging from approx. 1 to 5 μM in MCF7, for saccharinate complexes with mono- [54] and diphosphane ligands), [55] by Gimeno *et al*. (IC_{50} range between 2.81 and 25.42 μM in MCF7 and HepG2 cells, for complexes with modified amino acid esters and phosphine ligands), [56] and by McCann and Egan *et al*. (IC_{50} value between 0.9-3.8 μM in HepG2, for a 1,10-phenanthroline-5,6-dione complex, [57] for a 6-hydroxycoumarin-3-carboxilato complex, [58] and for a 4-oxy-3-nitro-coumarin silver(I) complex). [59]

Antibacterial activity

The antibacterial activities of the new complexes **2**-**6**, **9** and **10**, and their precursors (phosphazene ligands -**phos1** and **phos3**- and silver starting compounds) were tested against Gram-negative strains, *Escherichia coli* ATCC 10536 and *Pseudomonas aeruginosa* ATCC 15442, Gram-positive *Staphylococcus aureus* ATCC 11632 and against two MTBC strains, *M. tuberculosis* H37Rv ATCC 27294 and *M. bovis* BCG Pasteur. The Minimum Inhibitory Concentrations (MIC) obtained, and those of $AgNO_3$ and AgSD are listed in Table 6.

Table 6. Minimum Inhibitory Concentrations (μM) obtained for silver phosphazenes and their precursors against Gram+, Gram− and MTBC strains.

COMPOUND	*S. aureus (gram +)*	*E. Coli (gram −)*	*P. aeruginosa (gram −)*	*M. bovis BCG*	*M. tuber. H37Rv*
$[N_3P_3(NHCy)_6]$ **(phos-1)**	250	125	125	62.5	31.25
$[N_3P_3(NHCy)_6\{AgPPh_3\}_2](TfO)_2$ (**2**)	≤ 0.12	0.49	3.9	7.8	3.9
$[N_3P_3(NHCy)_6\{AgPPh_3\}_3](TfO)_3$ (**3**)	0.24	0.97	15.6	≤ 0.12	0.97
$[Ag(OTf)PPh_3]$	0.97	3.9	15.6	15.6	31.25
$[N_3P_3(NHCy)_6\{AgPPh_2Me\}_2](TfO)_2$ (**4**)	1.95	1.95	7,8	7.8	3.9
$[N_3P_3(NHCy)_6\{AgPPh_2Me\}_3](TfO)_3$ (**5**)	0.97	0.97	3.9	3.9	3.9
$[Ag(OTf)PPh_2Me]$	7.8	3.9	15.6	15.6	31.25
$[N_3P_3(NHCy)_6\{AgTPA\}_3](TfO)_3$ (**6**)	3.9	1.95	3.9	7.8	3.9
[Ag(OTf)TPA]	250	62.5	250	15.6	31.25
$[N_3P_3(NHCy)_3(NMe_2)_3]$ **(phos-3)**	62.5	125	125	15.6	15.6
$[N_3P_3(NHCy)_3(NMe_2)_3\{AgPPh_2Me\}_2](TfO)_2$ (**9**)	7.8	3.9	15.6	≤ 0.12	3.9
$[N_3P_3(NHCy)_3(NMe_2)_3\{AgPPh_2Me\}_3](TfO)_3$ (**10**)	7.8	1.95	15.6	≤ 0.12	3.9
$AgNO_3$ [a]	31.25	15.6	15.6	15.6	31.25
AgSD	44.8[b]	22.4[b]	13-90[c]	nd[d]	nd[d]

[a] Data measured by us, under the same conditions as the other compounds. [b] Data taken from reference [60] [c] Data taken from reference [61], where authors studied several strains of *P. aeruginosa*. MICs were transformed by us from μg/mL into μM. [d] Not determinated.

MIC values of tested metallophosphazenes (**2**-**6**, **9** and **10**) indicated that all of them exhibited excellent antibacterial activity against all bacterial strains used in this work,

being much higher than that of $AgNO_3$ and silver sulfadiazine (AgSD) for the entire range of bacteria studied, except **3**, **9** and **10**, which had a similar activity as $AgNO_3$ against *P. aeruginosa*. The MICs of all metallophosphazenes range from 0.12 to 15.6 μM. All metallophosphazenes exhibited much better activity than their phosphazene ligands and also than their silver precursors except **9** and **10**, which were as effective as their silver precursor [Ag(OTf)PPh_2Me] against *S. aureus*, *E. coli* and *P. aeruginosa*. **3** also exhibited a similar activity to its silver precursor, [Ag(OTf)PPh_3], against *P. aeruginosa*. Phosphazene ligands, **phos-1** and **phos-3**, were not active against *gram*+ and *gram*− strains but they were against the two MTBC strains, *M. tuberculosis* H37Rv and *M. bovis* BCG Pasteur, especially **phos-3**. Moreover, all metallophosphazenes and silver precursors showed better bactericidal properties against *S. aureus* and *E. coli* than against *P. aeruginosa* and, in general, also better than against the two MTBC strains. The best of these complexes were **2**, **3** and **5** with MIC values for *S. aureus* and *E. coli* between 0.12 – 0.97 μM (or 0.2 – 2.2 μg/mL if the molar mass is taken into account), which are among the lowest values found for any silver derivatives (see reference [2f] and references therein). **3**, **9** and **10** also exhibited an outstanding activity against *M. bovis* BCG Pasteur, see Table 6, MICs for the three complexes ≤ 0.12 μM (0.3 μg/mL for **3**, 0.2 μg/mL for **9** and 0.2 μg/mL for **11**). **3** also exhibited an excellent activity against *M. tuberculosis H37Rv* (see Table 6, 0.97 μM or 2.2 μg/mL).

As for the structure-activity relationships towards all bacterial strains in these metallophosphazenes, it can be said that the general trends observed for cytotoxic activity have been followed, in spite of not being so clear in some cases. The following can be concluded: (1) The antibacterial activity is higher in triphenylphosphane derivatives than in those with diphenylmethylphosphane or TPA (see Table 6; **3** is more toxic than **5** or **6**. There is an exception regarding *P. aeruginosa)*. (2) The antibacterial activity is also higher in those metallophosphazenes with **phos-1** than those with **phos-3** (see Table 6; **4** is more toxic than **9** and **5** more than **10**. There is an exception against *M. bovis and M. tuberculosis H37Rv,* which can be attributed to the fact that free phosphazene ligand **phos-3** was also active against the two MTBC strains). (3) There is not such a clear influence of the number of silvers linked to the phosphazene ring, as that observed for the cytotoxic activity (see Table 6, **5** is more toxic than **4** but the activity of **9** and **10** is similar against all bacterial strains used and **2** is even more toxic than **3** against *gram+* and *gram-*

strains). Remarkably, as in the case of cytotoxic properties, both metallophosphazenes **2** and **3** showed outstanding antibacterial activity against all strains studied. The broad spectrum antimicrobial efficacy of all these metallophosphazenes may be explained by the lability of the ligands in these silver (I) complexes. It was concluded that the antimicrobial properties of silver (I) complexes depend upon the fast rate of ligand exchange of the metal ion in the biological system (rather than solubility, charge or chirality), which correlates to the nature of the donor atoms coordinated to the silver. Weak Ag-O and Ag-N bonds play a key role to determine the wide spectrum antibacterial activity of Ag(I) complexes due to the easy substitution of the corresponding labile ligands with S- or N-donor sites of amino acids or nucleotides in bacteria [62]

3. Conclusions

Two multi-site (amino)cyclotriphosphazenes ligands, $[N_3P_3(NHCy)_6]$ (**phos-1**) and *nongem-trans*-$[N_3P_3(NHCy)_3(NMe_2)_3]$ (**phos-3**), were both prepared in high yield (>80%) from $[N_3P_3Cl_6]$ and *nongem-trans*-$[N_3P_3Cl_3(NMe_2)_3]$ (**phos-2**), respectively. The reaction of **phos-1** or **phos-3** with the silver complexes [Ag(OTf)L] (L= PPh_3, PPh_2Me or TPA) (TPA= 1,3,5-triaza-7-phosphaadamantane) (OTf= OSO_2CF_3), in dichloromethane and in different molar ratios 1:2 or 1:3, led to two series of the cationic metallophosphazenes $[N_3P_3(NHCy)_6\{AgL\}_n](TfO)_n$ (n=2, L= PPh_3 (**2**), PPh_2Me(**4**); n=3, L= PPh_3 (**3**), PPh_2Me(**5**), TPA(**6**)) and *nongem-trans*-$[N_3P_3(NHCy)_3(NMe_2)_3\{AgL\}_n](TfO)_n$ (n=2, L= PPh_3 (**7**), PPh_2Me(**9**); n=3, L= PPh_3 (**8**), PPh_2Me(**10**)). In all of them the silver groups “AgL” are coordinated to the nitrogen atoms of the phosphazene ring, whereby their number (two or three) depends on the molar ratio used. This type of coordination was confirmed by NMR spectroscopy and also, more specifically, by single-crystal X-ray diffraction for complexes **5**, **7** and **9**.

The cytotoxic activity of **2-6**, **9** and **10** have been studied against two tumour human cell lines, MCF7 (breast adenocarcinoma) and HepG2 (hepatocellular carcinoma). The IC_{50} values, which range from 1.6 to 5.5 μM for MCF7 and from 0.9 to 2.8 μM for HepG2, reveal an excellent cytotoxic activity for these metal complexes compared with their precursors and much higher than cisplatin, being their IC_{50} values among the lowest found in silver complexes. The structure-activity relationships towards both cell lines were clear. The cytotoxicity is higher in triphenylphosphane derivatives than in those with diphenylmethylphosphane or TPA and is higher in those with the phosphazene ligand

[$N_3P_3(NHCy)_6$] (**phos-1**) than in those with the phosphazene [$N_3P_3(NHCy)_3(NMe_2)_3$] (**phos-3**). A significant improvement in activity was also observed upon the rise in the number of silver atoms linked to the phosphazene ring. The same complexes were also tested against Gram-negative strains *Escherichia coli* and *Pseudomonas aeruginosa*, Gram-positive *Staphylococcus aureus* and against two MTBC strains, *M. tuberculosis* H37Rv and *M. bovis* BCG Pasteur. The MIC values, which range from 0.12 to 15.6 μM (some of them being the lowest found in silver complexes) indicated that all of them also exhibited excellent antibacterial activity against all bacterial strains used, being their activity much higher than those of $AgNO_3$ and silver sulfadiazine (AgSD). As for the structure-activity relationships, the general trends observed for cytotoxic activity are also followed for the bacterial growth inhibitions of these new metallophosphazenes. Thus, **2** and **3** are the most effective bacterial and cell growth inhibitors, which showed an outstanding antitumoral and antibacterial activity against all cell lines and bacterial strains studied. **9** and **10** also exhibited a remarkable activity against the two MTBC strains, especially for *M. bovis* BCG Pasteur. The outstanding biological activities of these complexes are worth studying further to determine action mechanisms and to elucidate the possibility of new biological targets.

4. Experimental Section

4.1. General Data. Infrared spectra were recorded in the range 4000-250 cm^{-1} on a PerkinElmer Spectrum-100 (ATR mode) FT-IR spectrometer. Carbon, hydrogen, nitrogen and sulfur analyses were performed using a PerkinElmer 240 B microanalyser. NMR spectra were recorded on a Brucker AV 400 spectrometer. Chemical shifts are quoted relative to $SiMe_4$ (TMS, ^1H and ^{13}C, external) and H_3PO_4 (85%) (^{31}P, external) and given in parts per million (ppm). FAB mass spectra were recorded using a Micromass Autospec spectrometer in positive-ion mode with m-nitrobenzyl alcohol (NBA) as matrix. Hexachlorocyclotriphosphazene, [$N_3P_3Cl_6$] (Stream Chemicals) was purified by recrystallization from hot hexane and dried in vacuum. Metal complexes [Ag(OTf)L] (L = PPh_3, PPh_2Me or TPA; OTf= OSO_2CF_3) were prepared according to published procedures. [37a, 38, 63] Culture medium, fetal bovine serum and cell culture reagents were obtained from Gibco and Corning (Biomol, Spain). Chemicals for the different assays were provided by VWR International Eurolab and Merck. Plastic material for the cytotoxicity assays were supplied by Fisher Scientific.

4.2. Synthesis and Spectroscopic Characterization Data.

Synthesis of [$N_3P_3(NHCy)_6$] (phos-1). To a solution of [$N_3P_3Cl_6$] (0.348 g, 1 mmol) in dry tetrahydrofuran (20 mL), a solution of NH_2Cy (4.6 mL, ρ=0,867g/mL, 40 mmol) in dry tetrahydrofuran (10 mL) was added slowly and dropwise. The mixture was stirred at room temperature for 12 h and then refluxed for 48 h. The precipitate of the amine hydrochloride was filtered off and the solvent was removed from the filtrate in vacuum. Addition of light petroleum (40-60 ºC) led to the precipitation of **phos-1** as a white solid. Successive additions of petroleum ether led to the precipitation of **phos-1** as a white solid.

Yield: 579 mg, 80%. Anal. Calcd (%) for $C_{36}H_{72}N_9P_3$ (723.94): C, 59.73; H, 10.02; N, 17.41. Found: C, 59.60; H, 9.90; N, 17.32. IR (ATR): 3405(w), 3360 (w), 3224 (w,br) cm^{-1} (N-H); 1186 (s, sh), 1178 (vs) cm^{-1} (P=N and C-N); 1092(vs), 1080 (s) cm^{-1} (P-NHR). $^{31}P\{^1H\}$ NMR ($CDCl_3$): δ = 14.44 (s, 3 P; $N_3\mathit{P}_3$ ring). ^1H NMR ($CDCl_3$): δ = 3.05 (m, 6H; NH-C*H*), 2.0 (br, 6H; N*H*), 1.94 (m, 12H; NH($C_6\mathit{H}_{11}$)), 1.65 (m, 12H; NH($C_6\mathit{H}_{11}$)), 1.50 (m, 6H; NH($C_6\mathit{H}_{11}$)), 1.26 (m, 12H; NH($C_6\mathit{H}_{11}$)), 1.10 (m, 18H; NH($C_6\mathit{H}_{11}$)). ^1H NMR (($CD_3)_2CO$): δ = 3.03 (m, 6H; NH-C*H*), 2.36 (br, 6H; N*H*), 1.97 (m, 12H; NH($C_6\mathit{H}_{11}$)), 1.67 (m, 12H; NH($C_6\mathit{H}_{11}$)), 1.54 (m, 6H; NH($C_6\mathit{H}_{11}$)), 1.28 (m, 12H; NH($C_6\mathit{H}_{11}$)), 1.14 (m, 18H; NH($C_6\mathit{H}_{11}$)). $^{13}C\{^1H\}$ NMR (($CD_3)_2CO$, APT): δ = 50.45 (s, 6C; NH-*C*H), 36.99, 26.6, 26.17 (s, 30C; *C*H_2). MS (FAB^+): m/z (%) = 725 (100) $[M+H]^+$ and peaks derived from the sequential loss of NH_2Cy and Cy.

Synthesis of *nongem-trans*-[$N_3P_3Cl_3(NMe_2)_3$] (phos-2). To a solution of [$N_3P_3Cl_6$] (3.48 g, 10 mmol) in dry tetrahydrofuran (30 mL), 60 mmol of $NHMe_2$ (30 mL of a solution 2.0 M in tetrahydrofuran) was added slowly and dropwise at 0ºC. The mixture was stirred for 1 h. When the mixture had reached room temperature, the precipitate of the amine hydrochloride was filtered off and the solvent was removed from the filtrate in vacuum affording an oil. Addition of hexane led to the precipitation of **phos-2** as a white solid.

Yield: 3.13 g, 84 %. Anal.Calcd (%) for $C_6H_{18}Cl_3N_6P_3$ (373.53): C 19.29, H 4.86, N 22.50; found: C 19.50, H 4.90, N 22.40. IR(ATR): 1193 (vs), 1172 (vs), 1146 (s, sh) cm^{-1} (P=N and C-N); 1059 (m) cm^{-1} (P-NR_2); 595 (s), 512 (vs), 495 (vs,br) cm^{-1} (P-Cl). $^{31}P\{^1H\}$ NMR ($CDCl_3$): δ= 28.65 (1P), 28.18 (2P) (AB_2 system, ^2J(P-P)= 40.6 Hz; N_3P_3 ring). ^1H NMR ($CDCl_3$): δ= 2.72 (m, *N*= 17.6 Hz, 6H; N($C\mathit{H}_3)_2$), 2.70 (m, *N*= 18.0 Hz, 12H; N($C\mathit{H}_3)_2$). $^{13}C\{^1H\}$ NMR ($CDCl_3$): δ = 36.40 (s, 2C; N($\mathit{C}H_3)_2$), 36.19 (s, 4C; N($\mathit{C}H_3)_2$). MS (FAB^+) m/z (%): 373 (100) $[M]^+$ and peaks derivated from the sequential loss of NMe_2 and Cl.

Synthesis of *nongem-trans*-[$N_3P_3(NHCy)_3(NMe_2)_3$] (phos-3). To a solution of *nongem-trans*-[$N_3P_3Cl_3(NMe_2)_3$] (0.374 g, 1 mmol) in dry tetrahydrofuran (20 mL), a solution of NH_2Cy (4.6 mL, 40 mmol) in dry tetrahydrofuran (10 mL) was added slowly and dropwise. The mixture was stirred at room temperature for 12 h and then refluxed for another 48 h. The precipitate of the amine hydrochloride was filtered off and the solvent was removed from the filtrate in vacuum. Addition of light petroleum (40-60 ºC) led to the precipitation of **phos-3** as a white solid. Successive additions of petroleum ether lead to the precipitation of **phos-3** as a white solid.

Yield: 477.4 mg, 85 %. Anal.Calcd (%) for $C_{24}H_{54}N_9P_3$ (561.67): C 51.32, H 9.69, N 22.44; found: C 51.30, H 10.0, N 22.0. IR(ATR): 3418(w), 3367(w), 3214 (w, br) cm^{-1} (N-H); 1180 (s, sh), 1171 (vs), 1140 (m) cm^{-1} (P=N and C-N); 1111(m, sh), 1096 (s), 1084 (vs) cm^{-1} (P-NHR); .$^{31}P\{^1H\}$ NMR ($CDCl_3$): δ= 20.96 (1P), 20.70 (2P) (AB_2 system, ^2J(P-P)= 44.3 Hz; N_3P_3 ring). ^1H NMR ($CDCl_3$): δ= 3.01 (br, 3H; NH-C*H*), 2.62 (m, *N*= 13.6 Hz, 18H; N(C*H*$_3$)$_2$),1.96 (m, br, 9H; N*H and* NH(C_6H_{11})), 1.64 (br, 6H; NH(C_6H_{11})), 1.53 (br, 3H; NH(C_6H_{11})), 1.26 (br, 6H; NH(C_6H_{11})), 1.09 (br, 9H; NH(C_6H_{11})). ^1H NMR (($CD_3)_2CO$): δ= 2.98 (br, 3H; NH-C*H*), 2.57 (m, *N*= 14 Hz, 18H; N(C*H*$_3$)$_2$), 2.41 (br, 3H; N*H*), 1.95 (m, br, 6H; NH(C_6H_{11})), 1.67 (m, 6H; NH(C_6H_{11})), 1.54 (m, 3H; NH(C_6H_{11})), 1.27 (m, 6H; NH(C_6H_{11})), 1.15 (m, 9H; NH(C_6H_{11})). $^{13}C\{^1H\}$ NMR (($CD_3)_2CO$, APT): δ = 50.38 (d, ^2J(P-C)= 10.3 Hz, 2C; NH-*C*H), 50.28 (d, ^2J(P-C)= 10.3 Hz, 1C; NH-*C*H), 37.60 (s, 6C; N(*C*H$_3$)$_2$), 36.81 (d, ^3J(P-C)= 8.4 Hz, 4C; *C*H$_2$), 36.73 (d, ^3J(P-C)= 11.3 Hz, 2C; *C*H$_2$), 26.58, 26.24, 26.17 (s, 9C; *C*H$_2$). MS (FAB^+) m/z (%): 562.5 (100) $[M+H]^+$ and peaks derived from the sequential loss of NMe_2 and NHCy.

Synthesis of [$N_3P_3(NHCy)_6Ag]_n(TfO)_n$ (1). To a solution of [$N_3P_3(NHCy)_6$] (144.8 mg, 0.2 mmol) in acetone (20 mL), AgTfO (51.4 mg, 0.2 mmol) was added. The mixture was stirred at room temperature for 30 min protected from the light. The solution was evaporated to *ca.* 1 mL. Addition of hexane led to the precipitation of **1** as a white solid.

Yield: 129.5 mg, 66%. Anal.Calcd (%) for $C_{37}H_{72}AgF_3N_9O_3P_3S$ (980.88): C, 45.31; H, 7.40; N, 12.85; S, 3.27. Found: C, 45.15; H, 8.01; N, 12.85; S, 3.60. IR (ATR): 3308 (m, br) cm^{-1} (N-H); 1076 (s) cm^{-1} (P-NHR). Other bands: 1297(s), 1226 (s, br), 1165 (m), 1081(s), 1030 (vs). $^{31}P\{^1H\}$ NMR ($CDCl_3$): δ = 10.39 (“t”, 1P), 8.43 (“d”, 2P) (AB_2 system, $^2J_{AB}$= 45.1 Hz; N_3P_3 ring). ^1H NMR ($CDCl_3$): δ = 3.15 (br, 6H; N*H*), 3.04 (br, 6H; NH-C*H*), 1.90 (m, 12H; NH(C_6H_{11})), 1.68 (br, 12H; NH(C_6H_{11})), 1.56 (m, 6H; NH(C_6H_{11})), 1.30-1.19 (m, 30H;

NH(C_6H_{11})). $^{19}F\{^1H\}$ NMR ($CDCl_3$, RT): δ = - 78.17 (s; SO_3CF_3). MS (FAB^+): m/z (%) = 1556 (3) $[[N_3P_3(NHCy)_6]_2Ag]^+$; 831 (3) $[M\text{-}SO_3CF_3]^+$, 725 (100) $[M\text{-}AgSO_3CF_3+H]^+$and peaks derived from the sequential loss of NH_2Cy and Cy.

Synthesis of $[N_3P_3(NHCy)_6\{AgL\}_2](TfO)_2$ (L= PPh_3(2), PPh_2Me(4)). To a solution of $[N_3P_3(NHCy)_6]$ (72.4 mg, 0.1 mmol) in dichloromethane (15 mL) was added Ag(OTf)L (0.2 mmol, 103.8 mg for **2** or 91.4 mg for **4**) and the mixture was stirred at room temperature for 30 min protected from the light. The solution was evaporated to *ca.* 1 mL. Addition of hexane led to the precipitation of **2** or **4** as white solids.

*Compound **2**:* Yield: 130.4 mg, 74%. Anal.Calcd (%) for $C_{74}H_{102}Ag_2F_6N_9O_6P_5S_2$ (1762.39):C, 50.43; H, 5.83; N, 7.15; S, 3.64. Found: C, 50.00; H, 5.30; N, 6.95; S, 3.60. IR (ATR): 3285 (m,br) cm^{-1} (N-H); 1074 (s) cm^{-1} (P-NHR). Other bands: 1284(m), 1237(s), 1221(vs), 1157(m), 1095(s), 1025 (vs). $^{31}P\{^1H\}$ NMR ($CDCl_3$, RT): δ = 16.90 (br s, 3P; N_3P_3 ring), 17.12 (dd, $^1J(^{109}Ag\text{-}P)$= 746.1 Hz, $^1J(^{107}Ag\text{-}P)$= 653.4 Hz, 2P; PPh_3). $^{31}P\{^1H\}$ NMR ($(CD_3)_2CO$, RT): δ = 16.11 (br s, 3P; N_3P_3 ring), 17.48 (dd, $^1J(^{109}Ag\text{-}P)$= 748.9 Hz, $^1J(^{107}Ag\text{-}P)$= 652.6 Hz, 2P; PPh_3). $^{31}P\{^1H\}$ NMR ($(CD_3)_2CO$, −80ºC): δ = 17.54 (“t”, 1P), 13.23 (“d”,2P) (AB_2 system, $^2J(P\text{-}P)$= 36.3 Hz; N_3P_3 ring), 17.51 (dd, $^1J(^{109}Ag\text{-}P)$= 740.6 Hz, $^1J(^{107}Ag\text{-}P)$= 641.3 Hz, 2P; PPh_3). ^1H NMR ($CDCl_3$, RT): δ = 7.54-7.40 (m, 30H; C_6H_5), 3.40 (br, 6H; N*H*), 3.00 (br, 6H; NH-C*H*), 1.90 (br, 12H; NH(C_6H_{11})), 1.66 (br, 12H; NH(C_6H_{11})), 1.54 (br, 6H; NH(C_6H_{11})), 1.26-1.09 (m, br, 30H; NH(C_6H_{11})). ^1H NMR ($(CD_3)_2CO$, RT): δ = 7.67-7.54 (m, 30H; C_6H_5), 4.03 (br, 6H; N*H*), 3.20 (br, 6H; NH-C*H*), 2.00 (br, 12H; NH(C_6H_{11})), 1.63 (br, 12H; NH(C_6H_{11})), 1.49 (br, 6H; NH(C_6H_{11})), 1.31 (m, br, 12H; NH(C_6H_{11})), 1.11 (m, br, 18H; NH(C_6H_{11})). ^1H NMR ($(CD_3)_2CO$, -80ºC): δ = 7.72-7.55 (m, 30H; C_6H_5), 4.65 (tbr, 2H; N*H*), 4.40 (br, 4H; N*H*), 3.13 (br, 6H; NH-C*H*), 2.00 (br, 12H; NH(C_6H_{11})), 1.65 (br, 6H; NH(C_6H_{11})), 1.53-1.41 (br, 12H; NH(C_6H_{11})), 1.29-0.56 (m, br, 30H; NH(C_6H_{11})). $^{13}C\{^1H\}$ NMR ($(CD_3)_2CO$, APT, RT): δ = 134.96 (d, $^2J(P\text{-}C)$= 16.1 Hz, 12C; P*Ph*$_3$), 132.58 (s, 6C; P*Ph*$_3$), 130.46 (d, $^1J(P\text{-}C)$= 41.9 Hz, 6C; P*Ph*$_3$),130.36 (d, $^3J(P\text{-}C)$= 11.0 Hz, 12C; P*Ph*$_3$), 121.99 (q, $^1J(C\text{-}F)$= 321.8 Hz, 2C; SO_3CF_3), 52.12 (s, 4C; NH-*C*H), 52.01 (s, 2C; NH-*C*H), 37.22, 26.14, 26.03 (s, 30C; *C*H_2). $^{19}F\{^1H\}$ NMR ($CDCl_3$, RT): δ = -77.84 (s; SO_3CF_3). MS (FAB^+): m/z (%) = 1613 (10) $[M\text{-}SO_3CF_3]^+$; 1464 (3) $[M+H\text{-}2SO_3CF_3]^+$; 1202 (8) $[M+H\text{-}2SO_3CF_3\text{-}PPh_3]^+$; 1093 (30) $[M\text{-}2SO_3CF_3\text{-}PPh_3\text{-}Ag]^+$, 831 (7) $[M\text{-}2SO_3CF_3\text{-}2PPh_3\text{-}Ag]^+$, 724 (100) $[M\text{-}2SO_3CF_3\text{-}2PPh_3\text{-}2Ag]^+$ and peaks derived from the sequential loss of NH_2Cy.

Compound ***4***: Yield: 142.5 mg, 87%. Anal.Calcd (%) for $C_{64}H_{98}Ag_2F_6N_9O_6P_5S_2$ (1638.25):C, 46.92; H, 6.03; N, 7.69; S, 3.91. Found: C, 46.45; H, 6.40; N, 7.35; S, 3.70. IR (ATR): 3301 (m,br) cm^{-1} (N-H); 1075 (vs) cm^{-1} (P-NHR). Other bands: 1275(m), 1239(s), 1221(vs), 1155(s), 1095 (s, sh), 1025 (vs). $^{31}P\{^1H\}$ NMR ($CDCl_3$, RT): δ = 16.22 (br s, 3P; N_3P_3 ring), -1.90 (dd, $^1J(^{109}Ag\text{-}P)$= 757.6 Hz, $^1J(^{107}Ag\text{-}P)$= 651.4 Hz, 2P; PPh_2Me). $^{31}P\{^1H\}$ NMR ($(CD_3)_2CO$, RT): δ = 16.24 (br s, 3P; N_3P_3 ring), -1.25 (dd, $^1J(^{109}Ag\text{-}P)$= 757.8 Hz, $^1J(^{107}Ag\text{-}P)$= 653.5 Hz, 2P; PPh_2Me). $^{31}P\{^1H\}$ NMR ($(CD_3)_2CO$, -80ºC): δ = 17.20 (“t”, 1P), 13.50 (“d”, 2P) (AB_2 system, $^2J_{P\text{-}P}$= 36.9 Hz; N_3P_3 ring), 0.64 (dd, $^1J(^{109}Ag\text{-}P)$= 753.9 Hz, $^1J(^{107}Ag\text{-}P)$= 652.4 Hz, 2P; PPh_2Me). ^1H NMR ($CDCl_3$, RT): δ = 7.60-7.41 (m, 20H; P*Ph*$_2$Me), 3.5 (br s, 6H; N*H*), 2.95 (br, 6H; NH-C*H*), 2.11 (d, ^2J(H-P)= 7.6 Hz, 6H; PPh_2*Me*), 1.85 (m, 12H; NH(C_6*H*$_{11}$)), 1.59 (m, 12H; NH(C_6*H*$_{11}$)), 1.42 (m, 6H; NH(C_6*H*$_{11}$)), 1.21 (m, 12H; NH(C_6*H*$_{11}$)), 1.06 (m, 18H; NH(C_6*H*$_{11}$)). ^1H NMR ($(CD_3)_2CO$, RT): δ = 7.80-7.51 (m, 20H; P*Ph*$_2$Me), 4.00 (br, 6H; N*H*), 3.13 (br, 6H; NH-C*H*), 2.20 (d, ^{2}J(H-P)= 7.6 Hz, 6H; PPh_2*Me*), 1.99 (m, 12H; NH(C_6*H*$_{11}$)), 1.64 (m, 12H; NH(C_6*H*$_{11}$)), 1.48 (m, 6H; NH(C_6*H*$_{11}$)), 1.32 (m, 12H; NH(C_6*H*$_{11}$)), 1.21-1.05 (m, 18H; NH(C_6*H*$_{11}$)). ^1H NMR ($(CD_3)_2CO$, −80ºC): δ = 7.85-7.54 (m, 20H; P*Ph*$_2$Me), 4.55 (br, 2H; N*H*), 4.20 (br, 4H; N*H*), 3.06 (br, 6H; NH-C*H*), 2.21 (br, 6H; PPh_2*Me*), 2.12 (br, 6H; NH(C_6*H*$_{11}$)), 1.90 (br, 6H; NH(C_6*H*$_{11}$)), 1.63 (br, 12H; NH(C_6*H*$_{11}$)), 1.51 (br, 6H; NH(C_6*H*$_{11}$)), 1.29-0.66 (m, br, 30H; NH(C_6*H*$_{11}$)). $^{13}C\{^1H\}$ NMR ($(CD_3)_2CO$, APT, RT): δ = 133.63 (d, ^{2}*J(P-C)*= 15.1 Hz, 8C; P*Ph*$_2$Me), 132.70 (d, ^{1}*J(P-C)*= 40.5 Hz, 4C; P*Ph*$_2$Me), 132.20 (s, 4C; P*Ph*$_2$Me), 130.16 (d, ^{3}*J(P-C)*= 10.4 Hz, 8C; P*Ph*$_2$Me), 122.03 (q, ^{1}*J(C-F)*= 310.7 Hz, 2C; SO_3CF_3),, 51.96 (s, 6C; NH-*C*H), 37.13, 26.21, 26.10 (s, 30C; *C*H_2), 12.94 (d, ^{1}*J(P-C)*= 23.4 Hz, 2C; PPh_2*C*H_3). $^{19}F\{^1H\}$ NMR ($CDCl_3$, RT): δ = -77.77 (s; SO_3CF_3). MS (FAB^+): m/z (%) = 1489 (2) $[M\text{-}SO_3CF_3]^+$; 1340 (1) $[M+H\text{-}2SO_3CF_3]^+$; 1140 (2) $[M+H\text{-}2SO_3CF_3\text{-}PPh_2Me]^+$; 1031 (90) $[M\text{-}2SO_3CF_3\text{-}PPh_2Me\text{-}Ag]^+$, 831 (25) $[M\text{-}2SO_3CF_3\text{-}2PPh_2Me\text{-}Ag]^+$, 725 (100) $[M\text{-}2SO_3CF_3\text{-}2PPh_2Me\text{-}2Ag+H]^+$ and peaks derived from the sequential loss of NH_2Cy.

Synthesis of $[N_3P_3(NHCy)_6\{AgL\}_3](TfO)_3$ (L= PPh_3(3), PPh_2Me(5), TPA(6)). To a solution of $[N_3P_3(NHCy)_6]$ (72.4 mg, 0.1 mmol) in dichloromethane (15 mL) (for **3** or **5**) or methanol for **6**, Ag(OTf)L (0.3 mmol, 155.7 mg for **3**, 137.1 mg for **5** or 124.2 mg for **6**) was added and the mixture was stirred at room temperature for 30 min protected from the light. The solution was evaporated to *ca.* 1 mL. Addition of hexane led to the precipitation of **3** or **5** as white solids. Addition of diethyl ether led to the precipitation of **6**.

*Compound **3**:* Yield: 178.0 mg, 78%. Anal.Calcd (%) for $C_{93}H_{117}Ag_3F_9N_9O_9P_6S_3$ (2281.61):C, 48.96; H, 5.17; N, 5.53; S, 4.22. Found: C, 49.00; H, 5.35; N, 4.95; S, 4.10. IR (ATR): 3267 (m,br) cm^{-1} (N-H); 1074 (vs) cm^{-1} (P-NHR). Other bands: 1282(m), 1236(s), 1219(s), 1154(s), 1095(s, sh), 1023 (vs). $^{31}P\{^1H\}$ NMR ($CDCl_3$, RT): δ = 18.38 (s, 3P; N_3P_3 ring), 16.53 (dd, $^1J(^{109}Ag\text{-}P)$= 761.7 Hz, $^1J(^{107}Ag\text{-}P)$= 662.0 Hz, 3P; PPh_3). ^1H NMR ($CDCl_3$, RT): δ = 7.49-7.42 (m, 45H; C_6H_5), 4.20 (br, 6H; N*H*), 3.02 (br, 6H; NH-C*H*), 1.86 (m, 12H; NH(C_6H_{11})), 1.46 (m, 12H; NH(C_6H_{11})), 1.34 (m, 6H; NH(C_6H_{11})), 1.25 (m, 12H; NH(C_6H_{11})), 1.04-0.85 (m, 18H; NH(C_6H_{11})). $^{13}C\{^1H\}$ NMR ($CDCl_3$, APT, RT): δ = 134.07 (d, $^2J(P\text{-}C)$= 11.0 Hz, 18C; P*Ph*$_3$), 131.40 (s, 9C; P*Ph*$_3$), 130.03 (s, 9C; P*Ph*$_3$), 129.40 (s, 18C; P*Ph*$_3$), 120.53 (q, $^1J(C\text{-}F)$= 320.2 Hz, 3C; SO_3CF_3), 51.89 (s, 6C; NH-*C*H), 36.60, 25.37, 25.12 (s, 30C; *C*H_2). $^{19}F\{^1H\}$ NMR ($CDCl_3$, RT): δ = -77.86 (s; SO_3CF_3). MS (FAB^+): m/z (%) = 2132 (1) $[M\text{-}SO_3CF_3]^+$, 1613 (3) $[M\text{-}2SO_3CF_3\text{-}PPh_3\text{-}Ag]^+$, 1464 (1) $[M\text{-}3SO_3CF_3\text{-}PPh_3\text{-}Ag+H]^+$, 1202 (1) $[M\text{-}3SO_3CF_3\text{-}2PPh_3\text{-}Ag+H]^+$, 1094 (100) $[M\text{-}3SO_3CF_3\text{-}2PPh_3\text{-}2Ag]^+$, 830 (20) $[M\text{-}3SO_3CF_3\text{-}3PPh_3\text{-}2Ag]^+$, 725 (35) $[M\text{-}3SO_3CF_3\text{-}3PPh_3\text{-}3Ag+H]^+$ and peaks derived from the sequential loss of NH_2Cy.

*Compound **5**:* Yield: 136.2 mg, 65%. Anal.Calcd (%) for $C_{78}H_{111}Ag_3F_9N_9O_9P_6S_3$ (2095.40):C, 44.71; H, 5.34; N, 6.02; S, 4.59. Found: C, 44.45; H, 5.70; N, 5.85; S, 4.40. IR (ATR): 3281 (m, br) cm^{-1} (N-H); 1076 (vs) cm^{-1} (P-NHR). Other bands: 1281(m), 1239(s), 1221(s), 1156(s), 1096 (m, sh), 1024 (vs). $^{31}P\{^1H\}$ NMR ($CDCl_3$, RT): δ = 18.57 (s, 3P; N_3P_3 ring), -2.78 (dbr, ^1J(Ag-P)= 718.0 Hz, 3P; PPh_2Me). ^1H NMR ($CDCl_3$, RT): δ = 7.58-7.44 (m, 30H; P*Ph*$_2$Me), 4.27 (br, 6H; N*H*), 2.96 (br, 6H; NH-C*H*), 2.11 (d, ^{2}J(H-P)= 7.6 Hz, 9H; PPh$_2$*Me*), 1.85 (m, 12H; NH(C_6H_{11})), 1.50 (m, 12H; NH(C_6H_{11})), 1.39 (m, 6H; NH(C_6H_{11})), 1.24 (m, 12H; NH(C_6H_{11})), 1.06-0.88 (m, 18H; NH(C_6H_{11})). ^1H NMR ($(CD_3)_2CO$, RT): δ = 7.77-7.51 (m, 30H; P*Ph*$_2$Me), 4.38 (br, 6H; N*H*), 3.15 (br, 6H; NH-C*H*), 2.20 (d, ^{2}J(H-P)= 7.6 Hz, 9H; PPh$_2$*Me*), 2.0 (m, 12H; NH(C_6H_{11})), 1.61 (m, 12H; NH(C_6H_{11})), 1.46 (m, 6H; NH(C_6H_{11})), 1.40-1.27 (m, 12H; NH(C_6H_{11})), 1.10-1.05 (m, 18H; NH(C_6H_{11})). $^{13}C\{^1H\}$ NMR ($(CD_3)_2CO$, APT, RT): δ = 133.56 (d, $^2J(P\text{-}C)$= 15.2 Hz, 12C; P*Ph*$_2$Me), 132.79 (d, $^1J(P\text{-}C)$= 39.3 Hz, 6C; P*Ph*$_2$Me), 132.16 (s, 6C; P*Ph*$_2$Me), 130.15 (d, $^3J(P\text{-}C)$= 10.4 Hz, 12C; P*Ph*$_2$Me), 121.95 (q, $^1J(C\text{-}F)$= 312.6 Hz, 3C; SO_3CF_3), 52.35 (s, 6C; NH-*C*H), 37.28, 26.15, 25.95 (s, 30C; *C*H_2), 12.95 (d, $^1J(P\text{-}C)$= 23.7 Hz, 3C; PPh$_2$*C*H$_3$). $^{19}F\{^1H\}$ NMR ($CDCl_3$, RT): δ = -77.87 (s; SO_3CF_3). MS (FAB^+): m/z (%) = 1598 (5) $[M\text{-}2SO_3CF_3\text{-}PPh_2Me+H]^+$, 1031 (5) $[M\text{-}3SO_3CF_3\text{-}2PPh_2Me\text{-}2Ag]^+$, 725 (100) $[M\text{-}3SO_3CF_3\text{-}3PPh_2Me\text{-}3Ag+H]^+$ and peaks derived from the sequential loss of NH_2Cy.

Compound ***6****:* Yield: 137.6 mg, 70%. Anal.Calcd (%) for $C_{57}H_{108}Ag_3F_9N_{18}O_9P_6S_3$ (1966.21):C, 34.82; H, 5.54; N, 12.82; S, 4.89. Found: C, 34.35; H, 5.80; N, 12.50; S, 4.55. IR (ATR): 3324 (m, br) cm^{-1} (N-H); 1080 (m) cm^{-1} (P-NHR). Other bands: 1267(m, sh), 1238(s), 1221(s), 1158(m), 1096 (m), 1026 (vs). $^{31}P\{^1H\}$ NMR (DMSO, RT): δ = 15.75 (s, 3P; N_3P_3 ring), -85.51 (s, br, 3P; TPA). ^1H NMR (DMSO, RT): δ = 4.59, 4.42 (AB system, ^2J(H-H)= 12.6 Hz, 18H; NC*H*$_2$N), 4.24 (s, br, 18H; NC*H*$_2$P), 3.41 (br, 6H; N*H*), 2.86 (br, 6H; NH-C*H*), 1.85 (m, br, 12H; NH(C_6H_{11})), 1.65 (m, br,, 12H; NH(C_6H_{11})), 1.53 (m, br, 6H; NH(C_6H_{11})), 1.15 (m, br, 30H; NH(C_6H_{11})). $^{19}F\{^1H\}$ NMR (DMSO, RT): δ = -77.72 (s; SO_3CF_3). MS (MALDI, ditranol): m/z (%) = 724 (100) [M-3SO_3CF_3-3TPA-3Ag+]$^+$ and peaks derived from the sequential loss of NH_2Cy.

Synthesis of *nongem-trans*-[N_3P_3(NHCy)$_3$(NMe$_2$)$_3${AgL}$_2$](TfO)$_2$ (L= PPh_3(7), PPh_2Me(9)). To a solution of *nongem,trans*-[N_3P_3(NHCy)$_3$(NMe$_2$)$_3$] (56.1 mg, 0.1 mmol) in dichloromethane (15 mL), Ag(OTf)L (0.2 mmol, 103.8 mg for **7** or 91.4 mg for **9**) was added. The mixture was stirred at room temperature for 30 min protected from the light. The solution was evaporated to *ca.* 1 mL. Addition of hexane led to the precipitation of **7** or **9** as white solids.

Compound ***7****:* Yield: 100.8 mg, 63%. Anal.Calcd (%) for $C_{62}H_{84}Ag_2F_6N_9O_6P_5S_2$ (1600.12):C, 46.54; H, 5.29; N, 7.88; S, 4.01. Found: C, 46.95; H, 5.45; N, 7.70; S, 4.00. IR (ATR): 3283 (m,br) cm^{-1} (N-H); 1078 (vs) cm^{-1} (P-N). Other bands: 1284(m), 1237(s), 1221(vs), 1157(m), 1095(s), 1025 (vs). $^{31}P\{^1H\}$ NMR ($CDCl_3$, RT): δ= 24.20 (“d”, 2P), 23.0 (“t”, 1P) (AB_2 system, $^2J_{P-P}$= 36.2 Hz; N_3P_3 ring), 16.58 (d, br, ^1J(Ag-P)= 671.5 Hz. ^1H NMR ($CDCl_3$, RT): δ= 7.51-7.48 (m, 30H; P*Ph*$_3$), 4.62 (br, 1H; N*H*), 4.44 (br, 2H; N*H*), 2.86 (br, 3H; NH-C*H*), 2.76-2.71 (m, 18H; N(CH_3)$_2$), 1.99-1.85 (m, 6H; NH(C_6H_{11})), 1.70 (m, 6H; NH(C_6H_{11})), 1.57-1.27 (m, 9H; NH(C_6H_{11})), 1.13-0.97 (m, 9H; NH(C_6H_{11})). $^{19}F\{^1H\}$ NMR ($CDCl_3$, RT): δ = -78.01 (s; SO_3CF_3). MS (FAB$^+$) m/z (%): 1600 (1) [M]$^+$, 1451 (1) [M-SO_3CF_3]$^+$, 1302 (1) [M-2SO_3CF_3+H]$^+$, 1189 (1) [M-SO_3CF_3-PPh_3]$^+$, 1040 (1) [M-2SO_3CF_3-PPh_3+H]$^+$, 933 (25) [M-2SO_3CF_3-PPh_3-Ag]$^+$, 562.5 (100) [M-2SO_3CF_3-2PPh_3-2Ag+H]$^+$ and peaks derived from the sequential loss of NMe_2 and NHCy.

Compound ***9***: Yield: 106.3 mg, 72%. Anal.Calcd (%) for $C_{52}H_{80}Ag_2F_6N_9O_6P_5S_2$ (1475.98):C, 42.31; H, 5.46; N, 8.54; S, 4.35. Found: C, 42.73; H, 5.60; N, 8.32; S, 4.16. IR (ATR): 3293 (m,br) cm^{-1} (N-H); 1077 (s) cm^{-1} (P-N). Other bands: 1281(m), 1235(s), 1221(s), 1155 (s), 1100 (m, sh), 1026(vs). $^{31}P\{^1H\}$ NMR ($CDCl_3$, RT): δ= 23.55 (br, 2P),

21.05 (br, 1P), (AB_2 system; N_3P_3 ring), -2.13 (dd, $^1J(^{109}Ag\text{-}P)$= 765.0 Hz, $^1J(^{107}Ag\text{-}P)$= 665.2 Hz, 2P; PPh_2Me). $^{31}P\{^1H\}$ NMR (CD_2Cl_2, −80 ºC): δ= 24.80 (“t”, 1P), 21.13 (“d”, 2P) (AB_2 system, $^2J_{P\text{-}P}$= 30.1 Hz;; N_3P_3 ring); 24.80 (“t”, 1P), 21.03 (“d”, 2P), (AB_2 system, $^2J_{P\text{-}P}$= 34.8 Hz; N_3P_3 ring), -0.81 (dd, $^1J(^{109}Ag\text{-}P)$= 728.6 Hz, $^1J(^{107}Ag\text{-}P)$= 696.0 Hz, 2P; PPh_2Me), -1.23 (dd, $^1J(^{109}Ag\text{-}P)$= 728.9 Hz, $^1J(^{107}Ag\text{-}P)$= 695.9 Hz, 2P; PPh_2Me). ^1H NMR ($CDCl_3$, RT): δ = 7.56-7.41 (m, 20H; P*Ph*$_2$Me), 4.24 (t, br, ^2J(P-H)= 9.6 Hz 1H; N*H*), 4.03 (br, 2H; N*H*), 2.84 (br, 3H; NH-C*H*), 2.71-2.66 (m, 18H; N(C*H*$_3$)$_2$), 2.11 (d, ^2J(P-H)= 7.6 Hz, 6H; PPh_2*Me*), 1.98-1.83 (m, 6H; NH(C_6H_{11})), 1.67 (m, 6H; NH(C_6H_{11})), 1.50-1.43 (br, 3H; NH(C_6H_{11})), 1.36-1.21 (m, 6H; NH(C_6H_{11})), 1.13-1.03 (m, 9H; NH(C_6H_{11})). ^1H NMR (CD_2Cl_2, −80 ºC): δ = 7.61-7.45 (m, 20H; P*Ph*$_2$Me), 4.31 (m, 2H; N*H*), 4.02 (t, ^2J(P-H)= 9.0 Hz, 1H; N*H*) 2.74 (br, 3H; NH-C*H*), 2.68-2.56 (m, 18H; N(C*H*$_3$)$_2$), 2.07 (d, ^2J(P-H)= 7.2 Hz, 6H; PPh_2*Me*), 2.07 (m, 3H; NH(C_6H_{11})), 1.60 (m, 6H; NH(C_6H_{11})), 1.49 (m, 6H; NH(C_6H_{11})), 1.35-0.93 (m, 15H; NH(C_6H_{11})). ^1H NMR ((CD_3)$_2$CO, RT): δ = 7.75-7.52 (m, 20H; P*Ph*$_2$Me), 4.27 (br, 3H; N*H*), 3.02 (br, 3H; NH-C*H*), 2.81 (m, *N*= 11.6 Hz, 18H; N(C*H*$_3$)$_2$), 2.20 (d, $^2J(P\text{-}H)$= 7.2 Hz, 6H; PPh_2*Me*), 1.99-1.89 (m, 6H; NH(C_6H_{11})), 1.67 (m, 6H; NH(C_6H_{11})), 1.54-1.49 (m, 3H; NH(C_6H_{11})), 1.37-1.26 (m, 6H; NH(C_6H_{11})), 1.24-1.03 (m, 9H; NH(C_6H_{11})). $^{13}C\{^1H\}$ NMR ((CD_3)$_2$CO, APT, RT): δ = 133.44 (d, $^2J(P\text{-}C)$= 15.0 Hz, 8C; P*Ph*$_2$Me), 132.91 (d, $^1J(P\text{-}C)$= 38.8 Hz, 4C; P*Ph*$_2$Me), 132.10 (s, 4C; P*Ph*$_2$Me), 130.16 (d, $^3J(P\text{-}C)$= 10.3 Hz, 8C; P*Ph*$_2$Me), 122.10 (q, $^1J(C\text{-}F)$= 315.8 Hz, 2C; SO_3CF_3), 51.87 (s, 3C; NH-*C*H), 38.05 (s, 6C; N(*C*H$_3$)$_2$), 37.11 (s, 2C; *C*H$_2$), 36.71 (d, $^3J(P\text{-}C)$= 13.2 Hz, 4C; *C*H$_2$), 26.27, 26.09 (s, 9C; *C*H$_2$), 12.72 (d, $^1J(P\text{-}C)$= 23.0 Hz, 2C; PPh_2CH_3). $^{19}F\{^1H\}$ NMR ($CDCl_3$, RT): δ = −77.88 (s; SO_3CF_3). MS (FAB^+): m/z (%) = 1327 (1) $[M\text{-}SO_3CF_3]^+$, 1178 (1) $[M\text{-}2SO_3CF_3\text{+H}]^+$, 1127 (1) $[M\text{-}SO_3CF_3\text{-}PPh_2Me]^+$, 978 (1) $[M\text{-}2SO_3CF_3\text{-}PPh_2Me\text{+H}]^+$, 869 (30) $[M\text{-}2SO_3CF_3\text{-}\ PPh_2Me\text{-Ag}]^+$, 562 (100) $[M\text{-}2SO_3CF_3\text{-}2PPh_2Me\text{-}2Ag]^+$ and peaks derived from the sequential loss of NMe_2 and NHCy.

Synthesis of *nongem-trans*-[N_3P_3(NHCy)$_3$(NMe$_2$)$_3${AgL}$_3$](TfO)$_3$ (L= PPh_3(8), PPh_2Me(10)). To a solution of *nongem,trans*-[N_3P_3(NHCy)$_3$(NMe$_2$)$_3$] (56.1 mg, 0.1 mmol) in dichloromethane (15 mL), Ag(OTf)L (0.3 mmol, 155.7 mg for **8** or 137.1 mg for **10**) was added. The mixture was stirred at room temperature for 30 min protected from the light. The solution was evaporated to *ca.* 1 mL. Addition of hexane led to the precipitation of **8** or **10** as white solids.

*Compound **8**:* Yield: 158.9 mg, 75%. Anal.Calcd (%) for $C_{81}H_{99}Ag_3F_9N_9O_9P_6S_3$ (2119.34):C, 45.90; H, 4.71; N, 5.95; S, 4.54. Found: C, 46.14; H, 5.05; N, 6.23; S, 4.32. IR (ATR): 3257 (m,br) cm^{-1} (N-H); 1079 (s) cm^{-1} (P-N). Other bands: 1282(m), 1236(s), 1219(s), 1154(s), 1095(s, sh), 1023 (vs). $^{31}P\{^1H\}$ NMR ($CDCl_3$, RT): δ = 24.27 (br, 3P; N_3P_3 ring), 16.19 (br, ^1J(Ag-P)= 671.5 Hz, 3P; PPh_3). ^1H NMR ($CDCl_3$, RT): δ = 7.46-7.42 (m, 45H; P*Ph*$_3$), 4.76 (br, 1H; N*H*), 4.54 (br, 2H; N*H*) 2.85 (br, 3H; NH-C*H*), 2.75 (m, 18H; N(C*H*$_3$)$_2$), 2.0-1.84 (m, 6H; NH(C_6H_{11})), 1.74 (m, 3H; NH(C_6H_{11})), 1.50-1.27 (m, 12H; NH(C_6H_{11})), 1.10-0.95 (m, 9H; NH(C_6H_{11})). $^{19}F\{^1H\}$ NMR ($CDCl_3$, RT): δ = -77.84 (s; SO_3CF_3). MS (FAB^+) m/z (%): 1450 (1) [M-2SO_3CF_3-PPh_3-Ag]$^+$,1301 (1) [M-3SO_3CF_3-PPh_3-Ag+H]$^+$, 1188 (1) [M-2SO_3CF_3-2PPh_3-Ag]$^+$, 1038 (1) [M-3SO_3CF_3-2PPh_3-Ag+H]$^+$, 931 (100) [M-3SO_3CF_3-2PPh_3-2Ag]$^+$, 561 (90) [M-3SO_3CF_3-3PPh_3-3Ag]$^+$ and peaks derived from the sequential loss of NMe_2 and NHCy.

*Compound **10**:* Yield: 135.3 mg, 70%. Anal.Calcd (%) for $C_{66}H_{93}Ag_3F_9N_9O_9P_6S_3$ (1933.13):C, 41.01; H, 4.85; N, 6.52; S, 4.98. Found: C, 41.40; H, 5.13; N, 6.96; S, 4.80. IR (ATR): 3269 (m,br) cm^{-1} (N-H); 1079 (s,br) cm^{-1} (P-N). Other bands: 1279(m), 1237(s), 1221(s), 1151(s), 1095(s, sh), 1025(vs). $^{31}P\{^1H\}$ NMR ($CDCl_3$, RT): δ = 24.07 (“d”, 2P), 23.08 (“t”, 1P) (AB_2 system, ^2J(P-P)= 33.1 Hz; N_3P_3 ring), -3.10 (br, 3P; PPh_2Me). ^1H NMR ($CDCl_3$, RT): δ = 7.55-7.41 (m, 30H; P*Ph*$_2$Me), 4.55 (t, ^2J(P-H)= 10.3 Hz, 1H; N*H*), 4.36 (t, br, ^2J(P-H)= 9.3 Hz, 2H; N*H*) 2.87 (br, 3H; NH-C*H*), 2.72 (m, *N*= 11.2 Hz, 18H; N(C*H*$_3$)$_2$), 2.09 (d, ^2J(H-P)= 7.6 Hz, 9H; PPh_2*Me*), 1.94 (m, 3H; NH(C_6H_{11})), 1.82 (m, 3H; NH(C_6H_{11})), 1.71 (m, 3H; NH(C_6H_{11})), 1.56 (m, 6H; NH(C_6H_{11})), 1.43-1.26 (m, 6H; NH(C_6H_{11})), 1.12-0.95 (m, 9H; NH(C_6H_{11})). ^1H NMR ($(CD_3)_2CO$, RT): δ = 7.75-7.51 (m, 30H; P*Ph*$_2$Me), 4.43 (m, 3H; N*H*), 3.02 (br, 3H; NH-C*H*), 2.82 (m, *N*= 11.6 Hz, 18H; N(C*H*$_3$)$_2$), 2.18 (d, ^2J(H-P)= 7.2 Hz, 9H; PPh_2*Me*), 2.00 (m, 3H; NH(C_6H_{11})), 1.89 (m, 3H; NH(C_6H_{11})), 1.65 (m, 6H; NH(C_6H_{11})), 1.50 (m, 3H; NH(C_6H_{11})), 1.34 (m, 6H; NH(C_6H_{11})), 1.22-1.03 (m, 9H; NH(C_6H_{11})).$^{13}C\{^1H\}$ NMR ($(CD_3)_2CO$, APT): δ = 133.43 (d, ^{2}*J(P-C)*= 15.2 Hz, 12C; P*Ph*$_2$Me), 133.05 (s, 6C; P*Ph*$_2$Me), 131.95 (s, 6C; P*Ph*$_2$Me), 130.09 (d, ^{3}*J(P-C)*= 10.2 Hz, 12C; P*Ph*$_2$Me), 122.06 (q, ^{1}*J(C-F)*= 321.2 Hz, 3C; SO_3CF_3), 51.95 (s, 2C; NH-*C*H), 51.87 (s, 1C; NH-*C*H), 38.12 (s, 4C; N(*C*H$_3$)$_2$), 38.06 (s, 2C; N(*C*H$_3$)$_2$), 37.15 (s, 2C; *C*H$_2$), 36.68 (d, ^{3}*J(P-C)*= 15.5 Hz, 4C; *C*H$_2$), 26.28, 26.09 (s, 9C; *C*H$_2$), 12.72 (d, ^{1}*J(P-C)*= 26.0 Hz, 3C; PPh_2*C*H$_3$). $^{19}F\{^1H\}$ NMR ($CDCl_3$, RT): δ = -77.80 (s; SO_3CF_3). MS (FAB^+) m/z (%): 1733 (1) [M-PPh_2Me]$^+$, 1327 (1) [M-2SO_3CF_3-PPh_2Me-Ag]$^+$, 1178 (1) [M-3SO_3CF_3-PPh_2Me-Ag+H]$^+$, 1127 (1) [M-2SO_3CF_3-2PPh_2Me -Ag]$^+$, 977 (1) [M-3SO_3CF_3-2PPh_2Me-Ag+H]$^+$,

869 (40) [M-3SO_3CF_3-2PPh_2Me-2Ag]$^+$, 562 (100) [M-3SO_3CF_3-3PPh_2Me-3Ag+H]$^+$ and peaks derived from the sequential loss of NMe_2 and NHCy.

4.3. X-Ray Structure Determinations

Crystals were mounted on glass fibres and transferred to the cold gas stream of a Bruker SMART 1000 CCD diffractometer. Measurements were made at -130°C. Absorption corrections were based on multi-scans. Structures were refined anisotropically using the program SHELXL-2017. [64] Hydrogen atoms of the NH groups were refined freely but with N–H distance restraints ("SADI"). Methyls were refined as idealised rigid groups allowed to rotate but not tip. Other hydrogens were included using a riding model starting from calculated positions. *Special features*: For **7**, two dichloromethane sites were identified and could be refined, but were not entirely satisfactory (high *U* values, significant residual electron density). Attempts to refine disorder models were unsuccessful. Accordingly, the program SQUEEZE (part of the PLATON suite) [65] was used to remove mathematically the effects of the solvent. The chemical formula and associated parameters are calculated using an idealised composition of two dichloromethane molecules per asymmetric unit. For **9**, the cyclohexyl group C51-56 is disordered over two positions. Appropriate restraints were employed to improve refinement stability, but the dimensions of disordered groups should be interpreted with caution. Dimensions of the hexane molecule, which lies across an inversion centre, are not entirely satisfactory, despite the use of restraints.

Deposition Numbers 1946587 and 1946588 contain the supplementary crystallographic data for this paper (for **7** and **9**, respectively). These data are provided free of charge by the joint Cambridge Crystallographic Data Centre and Fachinformationszentrum Karlsruhe Access Structures service www.ccdc.cam.ac.uk/structures.

4.4. Cell cultures.

To assess the cellular cytotoxicity and the antitumoral potential, human breast adenocarcinoma (MCF7) and human hepatocellular carcinoma (HepG2) epitelial cell lines were used. Both of them are commonly used in toxicology and in tumoral studies. Both were recognized as good experimental models, the first one, MCF7 cell line, due to its exquisite hormone sensitivity through expression of oestrogen receptor, making it an ideal model to study hormone response and a great breast cancer representative. [66] The second one, HepG2 cells, retained inducibility and activities of several phase I and phase

II xenobiotic metabolising enzymes. [67] Both cell lines were obtained from the American Type Culture Collection (ATCC, Manassas, VA, USA). MCF7 cells were cultured in monolayer in Dulbecco´s Minimum Essential Medium (DMEN) supplemented with 10% of fetal bovine serum, 100 U/mL penicillin and 100 µg/mL streptomycin (1%) and 2 mM L-glutamine (1%). The passages used for MCF7 are between 7-12. For HepG2 cells, Minimum Essential Medium (MEM) was used as main culture medium and similar nutrients and proportions above mentioned for MCF7. The passages we used were from 9-14. Cells were routinely grown at 37ºC and 5% CO_2 in a humidified atmosphere.

4.5. Citotoxicity assays.

For cytotoxicity assays, all the compounds analysed were dissolved in DMSO. In any case the DMSO concentration did not exceed 0.1% and appropriate controls of solvent were tested in all the experiments performed. Under the same conditions, but in water, cisplatin has been tested and compared to all the compounds studied.

The exposure concentrations for the silver complexes (**2-6**; **9** and **10**) were set from 0-8 µM, previous a wide range assayed (0-200 µM) to determine the specific spectrum to test and the compounds precipitation (data not shown). Different ranges of concentrations were tested based on their self-precipitation for phosphazene ligands, **phos-1** and **phos-2**, and the silver precursors. Thus, **phos1** was tested from 0 to 25 µM, and Ag(OTf)L (L=PPh_3, PPh_2Me, TPA) and **phos3** was assayed from 0 to 80 µM. MCF7 and HepG2 cells were seeded at a density of $8x10^4$ and $1x10^5$ cells/mL in 96 wells microplates and allowed to attach for 24 h prior to the addition of the compounds under study. In each assay, all the compounds were tested in sixtuplicate/microplate with three independent experiments being conducted to check the reproducibility and repetitivity of the results. The time of exposure of the silver complexes to the cell lines selected was 48h at 37ºC and 5% CO_2. At the same conditions, cisplatin (0-80 µM) has also been tested.

To evaluate the cell viability, two different biomarkers were carried out, Alamar Blue (AB) and Neutral Red Uptake (NRU) assays. In the AB assay, the system incorporates an oxidation-reduction (REDOX) indicator, assessing the mitochondrial ability to reduce resazurin into the fluorescent product resorufin. [68] Briefly, after 48h of the compounds exposure, AB medium was prepared by mixing cell culture medium with AB stock solution (resazurin sodium salt 5 mg/mL in phosphate buffer saline) in a 10:1 ratio (10% of final volume). Once prepared, 100 µL of the AB medium was added to each well containing

the cells exposed to the study compounds. The microplates were incubated at 37 °C for 2-3 h, and fluorescence was measured with the multimodal spectrophotometer Variouskan Lux (Thermo Scientific) with an excitation wavelength of 560 nm and an emission wavelength of 585 nm. As regards NRU, it is a suitable endpoint to determine viable cells. It is based on the ability of viable cells to incorporate and bind the supravital dye neutral red in the lysosomes. This assay was performed according to Repetto *et al*. [69] Briefly, after a 48 h exposure the medium with the complexes was removed and Neutral Red (NR) in fresh medium (1:100) was incorporated to each well (100µL) to be absorbed and concentrated in cell lysosomes. After 3h, the NR medium was removed, a formol-Ca_2 solution was added for 2 min and, afterwards, an acetic acid-ethanol-water mixture was also added for 15 min in continuous shaking, previous quantitative measurement at 540 nm with Variouskan Lux (Thermo Scientific).

For both biomarkers, cell viability was calculated using the ratio of the fluorescence/absorbance (depending on the biomarker) of treated cells to the fluorescence/absorbance of non-treated cells (control cells). All the results are expressed as mean ± standard deviation of the three independent experiments.

4.6. Antimicrobial activity assays.

Determination of MIC for Gram positive and Gram negative strains

The antibacterial activities of all compounds were tested against the Gram-negative strains *Escherichia coli* ATCC 10536, *Pseudomonas aeruginosa* ATCC 15442 and the Gram-positive *Staphylococcus aureus* ATCC 11632. Bacteria were stored as glicerol stocks at -80ºC and streaked onto Luria – Bertani plates prior to each experiment. Colonies from these newly prepared plates were inoculated into 5 ml LB media and the tubes were incubated at 37ºC. The overnight cultures were diluted to obtain a final concentration in the experiment of approximately 5 $x10^5$ cfus/mL. Stock solutions of each compound in DMSO were prepared at a concentration of 1 mM.

For quantitative determination of the susceptibility to all compounds, minimum inhibitory concentrations (MIC) were calculated by using 2-fold serial dilutions of compounds in 96 well microplate. MICs were performed according to the Clinical Laboratory Standards Institute (CLSI) methods, for Antimicrobial Susceptibility Testing. [70] The range of final concentrations tested spanned from 0.12 to 250 μM. Bacterial growth inhibition was assessed using 0.01% of resazurin added at the fifth hour of incubation at 37ºC. When a

colour change from blue to pink was seen in the antibiotic-free control wells, the MIC values were determined. The MIC is the lowest concentration of antimicrobial agent that prevents a colour change. Each experiment was performed twice.

Determination of MIC for Mycobacterium tuberculosis complex (MTBC) strains

The compounds were assayed against two MTBC strains, *M. tuberculosis* strain H37Rv ATCC 27294 and *M. bovis* BCG Pasteur. In this work, we also utilized *M. bovis* BCG, which is commonly used as a model organism for the study of *M. tuberculosis* because it is not virulent vaccine strain and the BCG genome shares a very high degree of similarity with that of *M. tuberculosis.* The anti-MTBC activity of all compounds was determined by the REMA (Resazurine Microtiter Assay) method according to Palomino *et al*. [71] Stock solutions of the tested compounds were prepared in DMSO and diluted in Middlebrook 7H9 (Difco) supplemented with oleic acid, albumin, dextrose and catalase (OADC enrichment-BBL/Becton–Dickinson) to obtain final drug concentration ranges of 0.12 - 250 μM of the *M. tuberculosis* strain H37Rv ATCC 27294 was cultured in Middlebrook 7H9 broth supplemented with OADC and 0.05% Tween 80. The concentration was adjusted by 5 x 10^5 UFC/mL and 100 μL of the inoculum was added to each well of 96-well microtiter plate together with 100 μL of the compounds. Samples were set up in duplicate. The plate was incubated at 37ºC under a normal atmosphere. After 7 days of incubation, 30 μL of 0.01% resazurin (solubilized in water) was added to each well, and the plate was reincubated 24 h. A change in color from blue to pink indicated the growth of bacteria and the MIC was defined as the lowest concentration of drug that prevented this change in color. For the Resazurin Solution, Resazurin sodium salt (Sigma-Aldrich) stock solution of 0.01 g was dissolved in 100 mL of sterile distilled water and sterilized by filtration.

Acknowledgments. This work was supported Ministerio de Economia y Competitividad (MINECO)-FEDER, under the project grant number MAT2017-84838-P, and Gobierno de Aragon-FEDER (Groups E47_17R and B25_17R, FEDER 2014-2020 "Construyendo Europa desde Aragón"), by the grant Proyecto Puente CTM2016-76304-C2-1-R and the grant for research group CTS996 PAIDI 2018, Consejería de Economía y Conocimiento de la Junta de Andalucía 2017, and project 2019-PPI1901 (VPPI-UPO). We thank Lucía Vallejo Valero for her contribution with the image design of the Table of Contents graphic.

Supporting Information. Tables containing details of data collection and structure refinement (Tables S1 and S2) and selected bond lengths and angles (Tables S3 and S4) for compounds **7** and **9**, ^{31}P and ^{1}H NMR spectra of compound **2** in DMSO measured over 48 hours, which is the time for the biological assays (Figures S1 and S2) and Table containing expected IC_{50} after 24 h to metallophosphazenes and their precursors exposure on MCF7 and HepG2 cells under microscope analysis (Table S5).

References

[1] Lansdown, A.B. A pharmacological and toxicological profile of silver as an antimicrobial agent in medical devices. *Adv. Pharmacol. Sci.* **2010**, *2010,* 1-16.

[2] For selected reviews about silver (I) complexes, see: (a) Klasen, H.J. Historical review of the use of silver in the treatment of burns. I. Early uses. *Burns* **2000**, *26*, 117-130. (b) Atiyeh, B.S.; Costagliola, M.; Hayek, S.N.; Dibo, S.A. Effect of Silver on Burn Wound Infection Control and Healing: Review of the Literature, Burns, **2007**, *33*, 139-148. (c) Azócar, M.I.; Gómez, G.; Levín, P.; Paez, M.; Muñoz, H.; Dinamarca, N. Review: Antibacterial behavior of carboxylate silver (I) complexes. *J. Coord. Chem.* **2014**, *67*, 3840-3853. (d) Medici, S.; Peana, M.; Crisponi, G.; Nurchi, V.M.; Lachowicz, J.I.; Remelli, M.; Zoroddu, M.A. Silver coordination compounds: a new horizon in medicine. *Coord. Chem. Rev.* **2016**, *327-328*, 349-359. (e) Sim, W.; Barnard, R.T.; Blaskovich, M.A.T.; Ziora. Z.M. Antimicrobial Silver in Medicinal and Consumer Applications: A Patent Review of the Past Decade (2007–2017). *Antibiotics* **2018**, *7*, **93**. (f) Liang, X.; Luan, S.; Yin, Z.; He, M.; He, C.; Yin, L.; Zou, Y.; Yuan, Z.; Li, L.; Song, X.; Lv, C.; Zhang, W. Recent advances in the medical use of silver complex. *Eur. J. Med. Chem*., **2018**, *157*, 62-80 and references therein.

[3] For selected reviews about silver nanoparticles, see: (a) Rai, M.; Yadav, A.; Gade, A.. Silver nanoparticles as a new generation of antimicrobials. *Biotechnol. Adv.* **2009**, *27*, 76 – 83. (b) Franci, G.; Falanga, A.; Galdiero, S.; Palomba, L.; Rai, M.; Morelli, G.; Galdiero, M. Silver Nanoparticles as Potential Antibacterial Agents. *Molecules* **2015**, *20*, 8856 –8874. (c) Roy, A. ; Bulut, O.; Some, S.; Mandal, A.K.; Yilmaz, M.D. Green synthesis of silver nanoparticles: biomolecule-nanoparticle organizations targeting antimicrobial activity. *RSC Adv.* **2019**, *9*, 2673-2702. (d) Liao, C.; Li, Y.; Tjong, S.C. Bactericidal and Cytotoxic Properties of Silver Nanoparticles. *Int. J. Mol. Sci.* **2019**, *20*, **449**. (e) Some, S.; Sen, I.K.; Mandal, A.; Aslan, T.; Ustun, Y.; Yilmaz, E.Ş.; Katı, A.;

Demirbas, A.; Mandal, A.K.; Ocsoy, I. Biosynthesis of silver nanoparticles and their versatile antimicrobial properties. *Mat. Res. Express* **2019***, 6,* **012001**.

[4] A monographic issue dedicated to bacterial resitance was published in (a) *Chem. Rev.* **2005**, *105*, 391-774; (b) *Nat. Rev. Microbiol.* **2010**, *8*, 836.

[5] Sierra, M.A.; Casarrubios, L.; de la Torre, M.C. Bio-Organometallic Derivatives of Antibacterial Drugs. *Chem. Eur. J.* **2019**, *25*, 7232-7242 and references therein.

[6] (a) Napoli, M. ; Saturnino, C.; Cianciulli, E. I.; Varcamonti, M.; Zanfardino, A.; Tommonaro, G.; Longo, P. Silver(I) *N*-heterocyclic carbene complexes: Synthesis, characterization and antibacterial activity. *J. Organomet. Chem.* **2013**, *725*, 46–53. (b) Kyros, L.; Banti, C. N.; Kourkoumelis, N.; Kubicki, M.; Sainis, I.; Hadjikakou, S. K. Synthesis, characterization, and binding properties towards CT-DNA and lipoxygenase of mixed-ligand silver(I) complexes with 2-mercaptothiazole and its derivatives and triphenylphosphine. *J. Biol. Inorg. Chem.* **2014**, *19*, 449–464.

[7] (a) Li, X.Z.; Nikaido, H.; Williams, K.E.J.B. Silver-resistant Mutants of Escherichia coli Display Active Efflux of Ag+ and Are Deficient. *Porins* **1997**, *179*, 6127-6132. (b) Gupta, A.; Matsui, K.; Lo, J.F.; Silver, S. Molecular basis for resistance to silver cations in Salmonella. *Nat. Med.* **1999,** *5*, 183-188. (c) Silver, S. Bacterial silver resistance: molecular biology and uses and misuses of silver compounds. *FEMS Microbiol. Rev*. **2003**, *27*, 341-353.

[8] Drake, P.L.; Hazelwood, K.J. Exposure-related health effects of silver and silver compounds: a review. *Ann. Occup. Hyg*. **2005,** *49,* 575-585.

[9] (a) Aulakh, J.K.; Lobana, T.S.; Sood, H.; Arora, D.S.; Smolinski, V.A.; Duff, C.E.; Jasinski, J.P. Synthesis, structures, and ESI-mass studies of silver(I) derivatives of imidazolidine-2-thiones: Antimicrobial potencial and biosafety evaluation. *J. Inorg. Biochem.* **2018**, *178*, 18-31. (b) Aulakh, J.K.; Lobana, T.S.; Sood, H.; Arora, D.S.; Kaur, R.; Singh, J.; Garcia-Santos, I.; Kaur, M.; Jasinski, J.P. Siver derivatives of multi-donor heterocyclic thioamides as antimicrobial/anticancer agents: unusual bio-activity against methicillin resitant *S. aureus, S. epidermidis,* and *E. faecalis* and human bone cancer *MG63* cell line. *RSC Adv.* **2019**, *9*, 15470-15487. (c) Aulakh, J.K.; Lobana, T.S.; Sood, H.; Arora, D.S.; Garcia-Santos, I.; Kaur, M.; Jasinski, J.P. Synthesis, structures, and novel antimicrobial activity of silver(I) halide complexes of imidazolidine-2-thiones.

Polyhedron, https://doi.org/10.1016/j.poly.2019.114235. (d) Banti, C.N.; Hadjikakou, S.K. Anti-proliferative and anti-tumor activity of silver (I) compounds. *Metallomics,* **2013**, *5*, 569-596 and references therein.

[10] For selected reviews concerning metallodrugs, see: (a) Pallavicini, P.; Dacarro, G.; Diaz-Fernandez, Y. A.; Taglietti, A. Coordination chemistry of surface-grafted ligands for antibacterial materials. *Coord. Chem. Rev.* **2014**, *275*, 37–53. (b) Medici, S.; Peana, M.; Nurchi, V.M.; Lachowicz, J.I.; Crisponi, G.; Zoroddu, M.A. Noble metals in medicine: Latest advances. *Coord. Chem. Rev.* **2015**, *284*, 329–350. (c) Klebowski, B.; Depciuch, J.; Parlinska-Wojtan, M. Applications of Noble Metal-Based Nanoparticles in Medicine. *Inter. J. Mol. Sci.* **2018**, *19*, **4031**. (d) del Solar, V.; Contel, M. Metal-based antibody drug conjugates. Potential and challenges in their application as targeted therapies in cancer. *J. Inorg. Biochem.* **2019**, *199*, 110780.

[11] (a) Liu, W.K.; Gust, R. Metal N-heterocyclic carbene complexes as potential antitumor metallodrugs, *Chem. Soc. Rev.* **2013**, *42*, 755-773. (b) Asekunowo, P.O.; Haque, R.A.; Razali, M.R. A comparative insight into the bioactivity of mono- and binuclear silver(I)-N-heterocyclic carbene complexes: synthesis, lipophilicity and substituent effect. *Rev. Inorg. Chem.* **2017**, *37*, 29-50. (c) Johnson, N.A.; Southerland, M.R. ; Youngs, W.J. Recent Developments in the Medicinal Applications of Silver-NHC Complexes and Imidazolium Salts. *Molecules* **2017**, *22*, 1263. (d) Mora, M.; Gimeno, M.C.; Visbal, R. Recent advances in gold–NHC complexes with biological properties. *Chem. Soc. Rev.* **2019**, *48*, 447-462.

[12] For a selected reviews, see: (a) Mark, J. E.; Allcock, H. R; West, R. Inorganic Polymers; Prentice Hall: Englewood Clifts, NJ, 1992; pp 61−141. (b) Allcock, H. R. Chemistry and Applications of Polyphosphazenes, Wiley-Interscience, New Jersey, 2003. (c) Gleria, M.; De Jaeger, R. Eds. Synthesis and Characterization of Polyphosphazenes (Vol. I). Applicative Aspects of Polyphosphazenes (Vol. II). Applicative Aspects of Cyclophosphazenes (Vol. III); Nova Science Publishers, Inc.: New York, 2004. (d) Allcock, H. R. The expanding field of polyphosphazene high polymers. *Dalton Trans.* **2016**, *45,* 1856−1862. (e) Rothemund, S.; Teasdale, I. Preparation of polyphosphazenes: a tutorial review. *Chem. Soc. Rev.* **2016**, *45*, 5200-5215. (f) Yeşilot, S.; Uslu, A. Stereochemical Aspects of Polyphosphazenes. *Polymer Reviews*, **2017**, *57*, 213–247. (g) Carriedo, G.A.; de la Campa, R.; Presa Soto, A. Polyphosphazenes –

Synthetically Versatile Block Copolymers(“Multi-Tool”) for Self-Assembly. *Eur. J. Inorg. Chem.* **2018**, 2484–2499.

[13] For selected and recient reviews, see: (a) Andrianov, A. K., Ed. Polyphosphazenes for Biomedical Applications; John Wiley & Sons, Inc.: Hoboken, NJ. **2009**. (b) Ullah, R.S.; Wang, L.; Yu, H.; Abbasi, N. M.; Akram, M.; ul-Adbin, Z.; Saleem, M.; Haroon, M.; Khan, R.U. Synthesis of polyphosphazenes with different side groups and various tactics for drug delivery. *RSC Adv.* **2017**, *7*, 23363-23391. (c) Wang, L.; Yang, Y-X.; Shi, X.; Mignani, S.; Caminade, A-M.; Majoral, J-P. Cyclotriphosphazene core-based dendrimers for biomedical applications: an update on recent advances. *J. Mater. Chem. B.* **2018**, *6,* 884-895. (d) Magiri, R.; Mutwiri, G.; Wilson, H.L. Recent advances in experimental polyphosphazene adjuvants and their mechanisms of action. *Cell and Tissue Research* **2018**, *374*, 465–471. (e) Teasdale, I. Stimuli-Responsive Phosphorus-Based Polymers. *Eur. J. Inorg. Chem.* **2019**, 1445–1456.

[14] See also: (a) Laurencin, C. T.; Norman, M. E.; Elgendy, H. M.; El-Amin, S. F.; Allcock, H. R.; Pucher, S. R.; Ambrosio, A. A. Use of polyphosphazenes for skeletal tissue regeneration. *J. Biomed. Mater. Res.* **1993**, *27*, 963–973. (b) Laurencin, C. T.; El-Amin, S. F.; Ibim, S. E.; Willoughby, D. A.; Attawia, M.; Allcock, H.R.; Ambrosio, A. A. A highly porous 3-dimensional polyphosphazene polymer matrix for skeletal tissue regeneration. *J. Biomed. Mater. Res.* **1996**, *30*, 133–138. (c) Langone, F.; Lora, S.; Veronese, F. M.; Caliceti, P.; Parnigotto, P. P.; Valenti, F.; Palma, G. Peripheral nerve repair using a poly(organo)phosphazene tubular prosthesis. *Biomaterials* **1995**, *16*, 347–353. (d) Veronese, F. M.; Marsilio, F.; Lora, S.; Caliceti, P.; Passi, P.; Orsolini, P. Polyphosphazene membranes and microspheres in periodontal diseases and implant surgery. *Biomaterials* **1999**, *20*, 91–98. (e) Henke, H.; Brüggemann, O.; Teasdale, I. Branched Macromolecular Architectures for Degradable, Multifunctional Phosphorus-Based Polymers. *Macromol. Rapid Commun.* **2017***, 38,* 1600644.

[15] (a) Andrianov, A.K.; Payne, L.G. Polymeric carriers for oral uptake of microparticulates. *Adv. Drug Delivery Rev.* **1998**, *34*, 155–170. (b) Andrianov, A.K.; Payne, L.G. Protein release from polyphosphazene matrices. *Adv. Drug Delivery Rev.* **1998**, *31*, 185–196. (c) Lakshmi, S.; Katti, D. S.; Laurencin, C. T.. Biodegradable polyphosphazenes for drug delivery applications. *Adv. Drug Delivery Rev*. **2003**, *55*, 467–482. (d) Akram, M.; Wang, L.; Yu, H.; Amer, W. A.; Khalid, H.; Abbasi, N. M.; Chen,

Y.; Saleem, M.; ul-Abdin, Z.; Tong, R. Polyphophazenes as anti-cancer drug carriers: From synthesis to application. *Prog. Polym. Sci.* **2014**, *39*, 1987–2009.

[16] (a) Duncan, R. Polymer conjugates for tumour targeting and intracytoplasmic delivery. The EPR effect as a common gateway? *Pharm. Sci. Technol. Today* **1999**, *2*, 441–449. (b) Maeda, H.; Wu, J.; Sawa, T.; Matsumura, Y.; Hori, K. Tumor vascular permeability and the EPR effect in macromolecular therapeutics: a review. *J. Control. Release* **2000**, *65*, 271–284. (c) Minko, T.; Kopeckova, P.; Kopecek, J. Efficacy of the chemotherapeutic action of HPMA copolymer-bound doxorubicin in a solid tumor model of ovarian carcinoma. *Int. J. Cancer* **2000**, *86,* 108–117. (d) Maeda, H. The enhanced permeability and retention (EPR) effect in tumor vasculature: the key role of tumor-selective macromolecular drug targeting. *Adv. Enzyme Regul.* **2001**, *41,* 189–207. (e) Maeda, H.; Sawa, T.; Konno, T. Mechanism of tumor-targeted delivery of macromolecular drugs, including the EPR effect in solid tumor and clinical overview of the prototype polymeric drug SMANCS. *J. Control. Release* **2001**, *74*, 47–61. (f) Kopecek, J., Kopeckova, P.; Minko, T.; Lu, Z.-R.; Peterson, C.M. Water soluble polymers in tumor targeted delivery. *J. Control. Release* **2001**, *74,* 147–158. (g) Maeda, H.; Fung, J.; Inutsuka, T.; Kitamoto, Y. Vascular permeability enhancement in solid tumor: various factors, mechanisms involved and its implications. *Int. Immunopharmacol.* **2003**, *3*, 319–328.

[17] Delgado, C.; Francis, G.E.; Fisher, D. The uses and properties of PEG-linked proteins. *Crit. Rev. Ther. Drug Carrier Sys.* **1992**, *9*, 249-304.

[18] (a) Jiménez, J.; Laguna, A.; Gascón, E.; Sanz, J.A.; Serrano, J.L.; Barberá, J.; Oriol, L. New Liquid Crystalline Materials Based on Two Generations of Dendronised Cyclophosphazenes. *Chem. Eur. J.* **2012**, *18*, 16801−16814. (b) Jiménez, J.; Pintre, I.; Gascón, E.; Sánchez-Somolinos, C.; Alcalá, R. ; Cavero, E.; Serrano, J.L.; Oriol, L. Photoresponsive Liquid-Crystalline Dendrimers Based on a Cyclotriphosphazene Core. *Macromol. Chem. Phys.* **2014**, *215*, 1551−1562. (c) Caminade, A.-M.; Ouali, A.; Hameau, A.; Laurent, R.; Rebout, C.; Delavaux-Nicot, B.; Turrin, C.-O.; Moineau Chane-Ching, K.; Majoral, J.-P. Cyclotriphosphazene, an old compound applied to the synthesis of smart dendrimers with tailored properties. *Pure Appl. Chem.* **2016**, *88*, 919-929. (d) Caminade, A.-M.; Hameau, A.; Majoral, J.-P. The specific functionalization of cyclotriphosphazenes for the synthesis of smart dendrimers. *Dalton Trans.* **2016**, *45*, 1810−1822.

[19] (a) Allcock, H. R.; Morozowich, N. L. Bioerodible polyphosphazenes and their medical potential. *Polym. Chem.* **2012**, *3*, 578–590. (b) Mignani, S.; El Kazzouli, S.; Bousmina, M. M.; Majoral, J. P. Dendrimer Space Exploration: An Assessment of Dendrimers/Dendritic Scaffolding as Inhibitors of Protein-Protein Interactions, a Potential New Area of Pharmaceutical Development. *Chem. Rev.* **2014**, *114*, 1327–1342. (c) Mukundam, V.; Dhanunjayarao, K.; Mamidala, R.; Venkatasubbaiah, K. Synthesis, characterization and aggregation induced enhanced emission properties of tetraarylpyrazole decorated cyclophosphazenes. *J. Mater. Chem. C*. **2016**, *4*, 3523–3530.

[20] (a) Allcock, H. R.; Desorcie, J. L.; Riding, G. H. The organometallic chemistry of phosphazenes. *Polyhedron* **1987**, *6*, 119-157. (b) Chandrasekhar, V.; Thomas, K. R. J. Coordination and organometallic chemistry of cyclophosphazenes and polyphosphazenes. *Appl. Organomet. Chem.* **1993**, *7*, 1-31. (c) Chandrasekhar, V.; Magendran, S-. Phosphazenes as scaffolds for the construction of multi-site coordination ligands. *Chem. Soc. Rev.,* **2001**, *30*, 193-203. (d) Chandrasekhar, V.; Krishnan, V. Advances in the chemistry of chlorocyclophosphazenes. *Adv. Inorg. Chem.,* **2002**, *53,* 159-211 (e) Steiner, A.; Zacchini, S.; Richards, P. I. From neutral iminophosphoranes to multianionic phosphazenates. The coordination chemistry of imino–aza-P(V) ligands. *Coord. Chem. Rev.* **2002**, *227*¸ 193-216. (f) Pertici, P.; Vitulli, G.; Gleria, M.; Facchin, G.; Milani, R.; Bertani, R. Metal-Containing Poly(Organophosphazenes). *Macromol. Symp.* **2006**, *235*, 98-114.

[21] (a) Lee, S.B.; Song, S.C.; Jin, J.I.; Sohn, Y.S. Synthesis and antitumor activity of polyphosphazene/methoxy-poly(ethylene glycol)/(diamine)platinum(II) conjugates. *Polymer Journal*, **1999**, *31*, 1247-1252. (b) Song, S.-C.; Lee, S.B.; Lee, B.H.; Ha, H.-W.; Lee, K.-T.; Sohn, Y.S. Synthesis and antitumor activity of novel thermosensitive platinum(II)-cyclotriphosphazene conjugates. *J. Control. Release* **2003**, *90*, 303-311. (c) Kim, Y.S.; Song, R.; Chung, H.C.; Jun, M.J.; Sohn, Y.S. Coordination modes vs. antitumor activity: synthesis and antitumor activity of novel platinum(II) complexes of N-substituted amino dicarboxylic acids. *J. Inorg. Biochem.* **2004**, *98*, 98-104. (d) Jun, Y.J.; Kim, J.I.; Jun, M.J.; Sohn, Y.S. Selective tumor targeting by enhanced permeability and retention effect. Synthesis and antitumor activity of polyphosphazene-platinum(II) conjugates. *J. Inorg. Biochem.* **2005**, *99*, 1593-1601. (e) Song, R.; Jun, Y.J.; Kim, J.I.;

Jin, C.; Sohn, Y. S. Synthesis, characterization, and tumor selectivity of a polyphosphazene-platinum(II) conjugate. *J. Control. Release* **2005**, *105*, 142-150. (f) Jadhav, V.B.; Jun, Y.J.; Song, J.H.; Park, M.K.; Oh, J.H.; Chae, S.W.; Kim, I.-S.; Choi, S.-J.; Lee, H.J.; Sohn, Y.S. A novel micelle-encapsulated platinum(II) anticancer agent. *J. Control. Release* **2010**, *147*, 144-150. (g) Avaji, P.G.; Joo, H.I.; Park, J.H.; Park, K.S.; Jun, Y.J.; Lee, H.J.; Sohn, Y.S. Synthesis and properties of a new micellar polyphosphazene-platinum(II) conjugate drug. *J. Inorg. Biochem.* **2014**, *140*, 45-52.

[22] Henke, H.; Kryeziu, K.; Banfic, J.; Theiner, S.; Körner, W.; Brüggemann, O.; Berger, W.; Keppler, B.K.; Heffeter, P.; Teasdale, I. Macromolecular Pt(IV) Prodrugs from Poly(organo)phosphazenes. *Macromol. Biosci.* **2016**, *16*, 1239-1249.

[23] (a) Wisian-Neilson, P.; García-Alonso, F.J. Coordination of poly(methylphenylphosphazene) and poly(dimethylphosphazene). *Macromolecules* **1993**, *26*, 7156-7160. (b) García-Alonso, F.J.; Wisian-Neilson, P. Backbone Coordination of Poly(alkyl/arylphosphazenes). *Polym. Prepr.* **1993**, *34(1),* 264-265. (c) Chen-Yang, Y.W.; Hwang, J.J.; Kau, J.Y. Polybisaminophosphazene-Silver Nitrate Complexes: Coordination and Properties. *J. Polym. Sci. Polym. Chem. Ed*. **1997**, *35*, 1023-1031. (d) Diefenbach, U.; Cannon, A. M.; Stromburg, B. E.; Olmeijer, D. L.; Allcock, H. R. Synthesis and metal coordination of thioether containing cyclo- and poly(organophosphazenes). *J. Appl. Polym. Sci.* **2000**, *78*, 650-661. (e) Itaya, T.; Inoue, K. Construction of hairy-rod coordination polymers with lamellar structure by self-assembling of hexakis(4-pyridylmethoxy)cyclotriphosphazene and silver alkylsulfonates. *Polyhedron* **2002**, *21*, 1573-1578. (f) Ainscough, E.W.; Brodie, A. M.; Depree, C. V.; Jameson, G. B.; Otter, C. A. Polymer Building Blocks: Self-Assembly of Silver(I) Cyclotriphosphazene Cationic Columns. *Inorg. Chem.* **2005**, *44*, 7325-7327. (g) Gonsior, M.; Antonijevic, S.; Krossing, I. Silver Complexes of Cyclic Hexachlorotriphosphazene. *Chem. Eur. J.* **2006**, *12*, 1997-2008. (h) Ainscough, E.W.; Brodie, A. M.; Davidson, R. J.; Otter, C. A. The first coordination polymer containing a chiral cyclotriphosphazene ligand. *Inorg. Chem. Commun.* **2008**, *11*, 171-174. (i) Chandrasekhar, V.; Narayanan, R.S. Metalation studies of 3- and 4-pyridyloxycyclophosphazenes: metallamacrocycles to coordination polymers. *Dalton Trans.* **2013***, 42,* 6619–6632. (j) Ainscough**,** E.W.; Brodie**,** A.M.; Davidson**,** R.J.; Jameson, G.B.; Otter, C.A. Flexible pyridyloxy-substituted cyclotetraphosphazene platforms linked by silver**(**I**).** *CrystEngComm* **2013**, *15*, 4379-4385.

(k) Gutowska, N.; Seliger, P.; Andrijewski, G. ; Siwy, M.; Małecka, M.; Kusz, J. Single and double crown macrocyclic derivatives of cyclotriphosphazene as receptors of silver(**I**) ions. *RSC Adv.* **2015**, *5*, 38435–38442. (l) Davarci, D. ; Gur, R.; Besli, S.; Senkuytu, E; Zorlu, Y. Silver(I) coordination polymers assembled from flexible cyclotriphosphazene ligand: structures, topologies and investigation of the counteranion effects. *Acta Cryst.* **2016**, *B72*, 344-356.

[24] (a) Richards, P.I.; Steiner, A. Cyclophosphazenes as Nodal Ligands in Coordination Polymers. *Inorg. Chem.* **2004***, 43,* 2810-2817 (b) Benson, M. A.; Zacchini, S.; Boomishankar, R.; Chan, Y.; Steiner, A. Alkylation and Acylation of Cyclotriphosphazenes. *Inorg. Chem.* **2007**, *46*, 7097-. (c) Richards, P. I.; Bickley, J. F.; Boomishankar, R.; Steiner, A. In situ recrystallisation of a coordination polymer with hemilabile linkers. *Chem. Commun.* **2008**, 1656-1658.

[25] (a) Jiménez, J.; Laguna, A.; Benouazzane, M.; Sanz, J.A.; Díaz, C.; Valenzuela, M.L.; Jones, P. G. Metallocyclo- and Polyphosphazenes Containing Gold or Silver: Thermolytic Transformation into Nanostructured Materials. *Chem. Eur. J.* **2009**, *15*, 13509- (b) Díaz, C.; Valenzuela, M.L.; Laguna, A.; Lavayen, V.; Jiménez, J.; Power, L.A.; O'Dwyer, C. Metallophosphazene Precursor Routes to the Solid-State Deposition of Metallic and Dielectric Microstructures and Nanostructures on Si and SiO_2. *Langmuir* **2010**, *26*(12), 10223–10233.

[26] (a) Wang, M.; Fu, J.; Huang, D; Zhang, C.; Xu, Q. Silver nanoparticles-decorated polyphosphazene nanotubes: synthesis and applications. *Nanoscale,* **2013***, 5,* 7913–7919. (b) Fu, J.; Wang, M.; Zhang, C.; Xu, Q.; Huang, X.; Tang, X. Controlled fabrication of noble metal nanoparticles loaded on the surfaces of cyclotriphosphazene-containing polymer nanotubes. *J Mater Sci.* **2012**, *47*, 1985–1991.

[27] Chandrasekhar, V.; Vivekanandan, K.; Nagendran, S.; Senthil Andavan, G.T.; Weathers, N.R.; Yarbrough, J.C.; Cordes, A.W. Cycloalkylaminocyclo- and Polyphosphazenes: X-ray Crystal Structures of gem-Tetrakis(cyclohexylamino)dichlorocyclotriphosphazene and Octakis(cyclopropylamino)-cyclotetraphosphazene. *Inorg. Chem.* **1998***, 37*, 6192-6198.

[28] Bickley, J.F.; Bonar-Law, R.; Lawson, G.T.; Richards, P.I.; Rivals, F.; Steiner, A.; Zacchini, S. Supramolecular variations on a molecular theme: the structural diversity of phosphazenes $(RNH)_6P_3N_3$ in the solid state. *Dalton Trans.,* **2003**, 1235-1244.

[29] (a) Ford, C.T.; Dickson, F.E.; Bezman, I.I. Positional and cis-trans Isomeric Dimethylaminotriphosphonitriles. The Use of ^1H Nuclear Magnetic Resonance in Configurational Analysis. *Inorg. Chem.,* **1964***,* *3*, 177-182. (b) Keat, R.; Shaw, R.A. Phosphorus-Nitrogen Compounds. Part IX. The Reaction of Dimethylamine with Hexachlorocyclotriphosphazatriene: The Replacement Pattern and the Structure of the Products. *J. Chem. Soc.,* **1965**, 2215.

[30] (a) Allen, C.W. Regio- and stereochemical control in substitution reactions of cyclophosphazenes. *Chem. Rev.* **1991**, *91*, 119-135. (b) Shaw, R.A. The Reactions of Halogenocyclophosphazenes with Nitrogenous Bases. *Z. Naturforsch. B,* **1976**, *31*, 641-667 (c) Krishnamurthy, S.S.; Sau, A.C.; Woods, M. Cyclophosphazenes. *Adv. Inorg. Chem. Radiochem.,* **1978**, *21*, 41-112.

[31] (a) Brandt, K.; Porwolik-Czomperlik, I.; Siwy, M.; Kupka, T.; Shaw, R.A.; Davies, D.B.; Hursthouse, M.B.; Sykara, G.D. Thermodynamic *vs* Supramolecular Effects in the Regiocontrol of the Formation of New Cyclotriphosphazene-Containing Chiral Ligands with 1,1'-Binaphthyl Units: Spiro *vs* Ansa Substitution at the N_3P_3 Ring. *J. Am. Chem. Soc*. **1997**, *119*, 12432-12440. (b) Wu, H.; Meng, S. ^{31}P NMR Analysis of Cyclotriphosphazenes. *Ind. Eng. Chem. Res.,* **1998**, *37*, 675-683. (c) McIntosh, M. B.; Hartle, T.J.; Allcock, H.R. Synthesis and Reactivity of Alkoxy, Aryloxy, and Dialkylamino Phosphazene Azides. *J. Am. Chem. Soc* **1999**, *121*, 884-885.

[32] In case of **phos-1** and **phos-2**, the characterization data agree with those reported in the literature. See references [27], [28] and [29]. In addition, selective decoupling NMR experiments and two-dimensional heteronuclear (HSQC ^1H-^{13}C) correlations were made by us to give a complete characterization and to assign the signals corresponding to cyclohexylamino units, specifically those of N*H* and NH-C*H*. See Experimental Section.

[33] (a) Ramachandran, K.; Allen, C.W. (Vinyloxy)chlorocyclotriphosphazenes. *Inorg. Chem.* **1983**, *22* 1445-1448. (b) Chen-Yang, Y.W.; Chien, W.S.; Chung, J.R. The synthesis, characterization and reaction of (propargyloxy)chlorocyclotriphosphazenes. *Polyhedron* **1989**, *8*, 1517-1522 (c) Uslu, A.; Güvenaltin, S. The investigation of structural

and thermosensitive properties of new phosphazene derivatives bearing glycol and amino acid. *Dalton Trans.* **2010**, *39*, 10685-10691.

[34] Jiménez, J.; Callizo, L.; Serrano, J.L.; Barberá, J.; Oriol, L. Mixed-Substituent Cyclophosphazenes with Calamitic and Polycatenar Mesogens*. Inorg. Chem.* **2017**, *56*, 7907−7921.

[35] The additional splitting and broadening are attributed to longer range coupling to the more distant phosphorus atoms and to quadrupole broadening by the adjacent nitrogen atom. See reference [**¡Error! Marcador no definido.**].

[36] (a) Lawrance, G. A. Coordinated Trifluoromethanesulfonate and Fluorosulfate. *Chem. Rev.* **1986**, *86*, 17-33. (b) Johnston, D.H.; Shriver, D.F. Vibrational Study of the Trifluoromethanesulfonate Anion: Unambiguous Assignment of the Asymmetric Stretching Modes. *Inorg. Chem*., **1993**, *32*, 1045-1047.

[37] (a) Bardaji, M.; Crespo, O.; Laguna, A.; Fischer, A.K. Structural characterization of silver (I) complexes [Ag(O_3SCF_3)(L)] (L=PPh_3, PPh_2Me, SC_4H_8) and [AgL_n](CF_3SO_3) (n=2–4), (L=PPh_3, PPh_2Me)*. Inorg. Chim. Acta,* **2000**, *304*, 7-16. (b) Jiménez, J.; Laguna, A.; Benouazzane, M.; Sanz, J.A.; Díaz, C.; Valenzuela, M.L.; Jones, P.G. Metallocyclo- and Polyphosphazenes Containing Gold or Silver: Thermolytic Transformation into Nanostructured Materials. *Chem. Eur. J.* **2009**, *15*, 13509-13520.

[38] (a) Contel, M.; Jiménez, J.; Jones, P.G.; Laguna, A.; Laguna, M. Mesitylgold complexes: synthesis and reactivity; crystal structure of [{(Ph_3P)Au(μ-mes)Ag(tht)}$_2$][SO_3CF_3]$_2$(mes = mesityl, tht = tetrahydrothiophene). *J. Chem. Soc. Dalton Trans.,* **1994**, *17*, 2515-2518 (b) Terroba, R.; Hursthouse, M.B.; Laguna, M.; Mendia, A. Unexpected diastereoisomeric-trimers in the crystalline structure of triflatetriphenylphosphinesilver(I). *Polyhedron*, **1999**, *18*, 807-810.

[39] Mohr, F.; Falvello, L. R.; Laguna, M. A Silver(I) Coordination Polymer Containing Tridentate *N*- and *P*- Coordinating 1,3,5-Triaza-7-phosphaadamantane (PTA) Ligands. *Eur. J. Inorg. Chem.* **2006**, 3152–3154.

[40] The two sets of resonances of two AB_2 spin systems corresponding to the phosphazene phosphorus atoms are marked in Figure 4a with symbols (• and ♦).

[41] The two sets of two doublets corresponding to the phosphane phosphorus atoms are marked in Figure 4a with symbols (***** and **o**).

[42] (a) Cingolani, A.; Effendy, Marchetti, F.; Pettinari, C.; Skelton, B.W.; White, A.H. Synthesis and structural systematics of mixed triphenylphosphine/imidazole base adducts of silver(I) oxyanion salts. *J. Chem. Soc*., *Dalton Trans*. **1999**, 4047–4055. (b) Bardají, M.; Barrio, M.; Espinet, P. Photosensitive azobispyridine gold(I) and silver(I) complexes. *Dalton Trans*. **2011**, *40*, 2570-2577. (c) Johnson, A.; Marzo, I.; Gimeno, M.C. Ylide Ligands as Building Blocks for Bioactive Group 11 Metal Complexes. *Chem. Eur. J.* **2018**, *24*, 11693 –11702.

[43] Lawson, G.T.; Rivals, F.; Tascher, M.; Jacob, C.; Bickley, J.F.; Steiner, A. *Cis*-Trihydrogen cyclotriphosphazenates—acidic anions in strongly basic media. *Chem. Commun.*, **2000**, 341–342.

[44] (a) Schmidpeter, A.; Blanck, K.; Ahmed, F.R. Bis[cyclotri(λ^5-phosphazane)dienethionato]-Ni^{II}, -Pd^{II} and –Pt^{II} Complexes and Their Structure. *Angew. Chem. Int. Ed. Engl.* **1976**, *15*, 488-489. (b) Allen, R.W.; O'Brien, J.P.; Allcock, H.R. Crystal and Molecular Structure of a Platinum-Cyclophosphazene Complex: cis-Dichloro[octa-(methylamino)cyclotetraphosphazene-N,N "]platinum(11 *J. Am. Chem. Soc.* **1977**, *99*, 3987- 3991. (c) Thomas, K.R.J.; Chandrasekhar, V.; Pal, P.; Scoot, S.R.; Hallford, R.; Cordes, A.W. Unusual Tridentate N_3 Capping Coordination Behavior of Hexakis(3,5-dimethylpyrazolyl)cyclotriphosphazene, $N_3P_3(3,5\text{-}Me_2Pz)_6$: Synthesis, Spectroscopy, and Electrochemistry of Mono- and Dinuclear Copper(II) Complexes and the X-ray Structure of $N_3P_3(3,5\text{-}Me_2Pz)_6$*$CuCl_2$. *Inorg. Chem.* **1993**, *32*, 606-611. (d) Çhandrasekhar, V.; Krishnan, V.; Steiner, A.; Bickley, J. Cyclotriphosphazene Hydrazides as Efficient Multisite Coordination Ligands. η^3-fac-non-geminal-N_3 Coordination of spiro-$N_3P_3[O_2C_{12}H_8][N(Me)NH_2]_4$ (L) in L_2CoCl_3 and $L_2M(NO_3)_2$ (M=Ni, Zn, Cd). *Inorg. Chem.* **2004***, 43,* 166-172. (e) Richards, P.I.; Lawson, G.T.; Bickley, J.F.; Robertson, C.M.; Iggo, J.A.; Steiner, A. Polyanionic Ligand Platforms for Methyl- and Dimethylaluminum Arrays. *Inorg. Chem.* **2019**, *58*, 3355−3363.

[45] (a) Trotter, J.; Whitlow, S.H. Crystal structure of bis(octamethylcyclotetraphosphonitrilium) tetrachlorocobaltate(II), $[(NPMe_2)_4H]_2CoCl_4$. *J. Chem. Soc. A*, **1970**, 460-464. (b) Chandrasekaran, A. A salt of a protonated (amino)spirocyclic cyclotriphosphazene. *Acta Cryst.* **1994**, *C50*, 1692-1694. (c) Richards,

P.I.; Benson, M.A.; Steiner, A. *In situ* complexation of lithium chloride by amphiprotic cyclophosphazenes. *Chem. Commun.*, **2003**, 1392-1393. (d) Craven, M.; Yahya, R.; Kozhevnikova, E.; Boomishankar, R.; Robertson, C. M.; Steiner, A.; Kozhevnikov, I. Novel polyoxometalate–phosphazene aggregates and their use as catalysts for biphasic oxidations with hydrogen peroxide. *Chem. Commun.* **2013**, *49*, 349-351. (e) Benson, M.A.; Zacchini, S.; Boomishankar, R.; Chan, Y.; Steiner, A. Alkylation and Acylation of Cyclotriphosphazenes. *Inorg. Chem.* **2007**, *46*, 7097-7108. (f) Benson, M.A.; Ledger, J.; Steiner, A. Zwitterionic Phosphazenium Phosphazenate Ligands. *Chem. Commun.* **2007**, 3823−3825.

[46] (a) Craig, D.P.; Maccoll, A.; Nyholm, R.S.; Orgel, L.E.; Sutton, L.E. Chemical bonds involving *d*-orbitals. Part I. *J. Chem. Soc.* **1954**, 332-353. (b) Searle, H.T.; Dyson, J.; Ranganathan, T.N.; Paddock, N.L. Preparation and donor properties of the cyclic methylphosphazenes. *J. Chem. Soc., Dalton Trans.,* **1975**, 203-208. (c) Gallicano, K.D.; Paddock, N.L.; Tetting, S.J., Trotter, J. 1-Pyrazolylphosphazenes and their metal complexes. *J. Inorg. Nucl. Chem. Lett.* **1979**, *15*, 417-420.

[47] (a) Ott, I.; Koch, T.; Shorafa, H.; Bai, Z.; Poeckel, D.; Steinhilber, D.; Gust, R. Synthesis, cytotoxicity, cellular uptake and influence on eicosanoid metabolism of cobalt–alkyne modified fructoses in comparison to auranofin and the cytotoxic COX inhibitor Co-ASS. *Org. Biomol. Chem*., **2005**, *3*, 2282-2286. (b) Ortego, L.; Cardoso, F.; Martins, S.; Fillat, M.F.; Laguna, A.; Meireles, M.; Villacampa, M.D.; Gimeno, M.C. Strong inhibition of thioredoxin reductase by highly cytotoxic gold(I) complexes. DNA binding studies. *J. Inorg. Biochem*. **2014**, *130,* 32-37.

[48] Goitia, H.; Nieto, Y.; Villacampa, M.D.; Kasper, C.; Laguna, A.; Gimeno, M.C. Antitumoral Gold and Silver Complexes with Ferrocenyl-Amide Phosphines. *Organometallics,* **2013**, *20*, 6069-6078.

[49] (a) Poyraz, M.; Banti, C. N.; Kourkoumelis, N.; Dokorou, V.; Manos, M. J.; Simcic, M.; Golic-Grdadolnik, S.; Mavromoustakos, T.; Giannoulis, A. D.; Verginadis, I. I.; Charalabopoulos, K.; Hadjikakou, S. K. Synthesis, structural characterization and biological studies of novel mixed ligand Ag(I) complexes with triphenylphosphine and aspirin or salicylic acid. *Inorg. Chim. Acta,* **2011**, *375*, 114–121. (b) Banti, C. N.; Giannoulis, A. D.; Kourkoumelis, N.; Owczarzak, A. M.; Poyraz, M.; Kubicki, M.; Charalabopoulos, K.; Hadjikakou, S. K. Mixed ligand–silver(I) complexes with anti-

inflammatory agents which can bind to lipoxygenase and calf-thymus DNA, modulating their function and inducing apoptosis. *Metallomics,* **2012**, *4*, 545–560.

[50] Galal, S. A.; Hegab, K. H., Kassab, A. S., Rodriguez, M. L., Kerwin, S. M., El-Khamry, A. M. A., El Diwani, H. I. New transition metal ion complexes with benzimidazole-5-carboxylic acid hydrazides with antitumor activity. *Eur. J. Med. Chem.,* **2009**, *44*, 1500–1508.

[51] Teyssot, M.-L.; Jarrousse, A.-S.; Manin, M.; Chevry, A.; Roche, S.; Norre, F.; Beaudoin, C.; Morel, L.; Boyer, D.; Mahiou, R.; Gautier, A. Metal-NHC complexes: a survey of anti-cancer properties. *Dalton Trans.,* **2009**, 6894–6902.

[52] Haque, R.A.; Budagumpi, S.; Zetty Zulikha, H.; Hasanudin, N.; Khadeer Ahamed, M.B.; Abdul Majid, A.M.S. Silver(I)-N-heterocyclic carbene complexes of nitrile-functionalized imidazol-2-ylidene ligands as anticancer agents, *Inorg. Chem. Commun*. **2014**, *44*, 128-133.

[53] (a) Hackenberg, F.; Lally, G.; Müller-Bunz, H.; Paradisi, F.; Quaglia, D.; Streciwilk, W.; Tacke, M. Novel symmetrically p-benzyl-substituted 4,5-diaryl-imidazole N-heterocyclic carbene-silver(I) acetate complexes. Synthesis and biological evaluation, *J. Organomet. Chem.* **2012**, 717, 123-134. (b) Hackenberg, F.; Lally, G.; Müller-Bunz, H.; Paradisi, F.; Quaglia, D.; Streciwilk, W.; Tacke, M. Synthesis and biological evaluation of N-heterocyclic carbenesilver(I) acetate complexes derived from 4,5-ditolyl-imidazole, *Inorg. Chim. Acta.* **2013**, *395*, 135-144. (c) Streciwilk, W.; Cassidy, J.; Hackenberg, F.; Müller-Bunz, H.; Paradisi, F.; Tacke, M. Synthesis, cytotoxic and antibacterial studies of p-benzyl-substituted NHC-silver(I) acetate compounds derived from 4,5-di-p-diisopropylphenyl- or 4,5-di-p-chlorophenyl-1H-imidazole. *J. Organomet. Chem.* **2014**, *749*, 88-99.

[54] Yilmaz, V.T.; Gocmen, E.; Icsel, C.; Cengiz, M.; Susluer, S.Y.; Buyukgungor, O. Synthesis, crystal structures, in vitro DNA binding, antibacterial and cytotoxic activities of new di- and polynuclear silver(I) saccharinate complexes with tertiary monophosphanes. *J. of Photochemistry and Photobiology B: Biology*, **2014**, *131*, 31-42.

[55] Yilmaz, V.T.; Gocmen, E.; Icsel, C.; Gengiz, M.; Susluer, S.Y.; Buyukgungor, O. Di- and polynuclear silver(I) saccharinate complexes of tertiary diphosphane ligands:

synthesis, structures, in vitro DNA binding, and antibacterial and anticancer properties. *J. Biol. Inorg. Chem.*, **2014**, *19*, 29-44.

[56] Ortego, L.; Meireles, M.; Kasper, C.; Laguna, A.; Villacampa, M.D.; Gimeno, M.C. Group 11 complexes with amino acid derivatives: Synthesis and antitumoral studies. *J. Inorg. Biochem.*, **2016**, *156*, 133-144.

[57] (a) McCann, M.; Coyle, B.; McKay, S.; McCormack, P.; Kavanagh, K.; Devereux, M.; McKee, V.; Kinsella, P.; O'Connor, R.; Clynes, M. Synthesis and X-ray crystal structure of $[Ag(phendio)_2]ClO_4$ (phendio = 1,10-phenanthroline-5,6-dione) and its effects on fungal and mammalian cells. *BioMetals*, **2004**, *17*, 635–645. (b) Deegan, C.; Coyle, B.; McCann, M.; Devereux, M.; Egan, D.A. *In vitro* anti-tumour effect of 1,10-phenanthroline-5,6-dione (phendione), $[Cu(phendione)_3](ClO_4)_2 \cdot 4H_2O$ and $[Ag(phendione)_2]ClO_4$ using human epithelial cell lines. *Chem.-Biol. Interact.* **2006**, *164*, 115–125.

[58] Thati, B.; Noble, A.; Creaven, B. S.; Walsh, M.; McCann, M.; Kavanagh, K.; Devereux, M.; Egan, D. A. RETRACTED: *In vitro* anti-tumour and cyto-selective effects of coumarin-3-carboxylic acid and three of its hydroxylated derivatives, along with their silver-based complexes, using human epithelial carcinoma cell lines. *Cancer Lett.* **2007**, *248*, 321–331.

[59] Thati, B.; Noble, A.; Creaven, B.S.; Walsh, M.; McCann, M.; Devereux, M.; Kavanagh, K.; Egan, D.A. Role of cell cycle events and apoptosis in mediating the anti-cancer activity of a silver(I) complex of 4-hydroxy-3-nitro-coumarin-bis(phenanthroline) in human malignant cancer cells. *Eur. J. Pharmacol.* **2009**, *602*, 203–214.

[60] Yilmaz, V.T.; Icsel, C.; Batur, J.; Aydinlik, S.; Sahinturk, P.; Aygun, M. Structures and biochemical evaluation of silver(I) 5,5-diethylbarbiturate complexes with bis(diphenylphosphino)alkanes as potential antimicrobial and anticancer agents. *Eur. J. Med. Chem.*, **2017**, *139*, 901-916.

[61] Von Silva-Tarouca, M.S.E.; Wolf, G.; Mueller, R.S. Determination fo mínimum inhibitory concentrations for silver sulfadiazine and other topical antimicrobial agents against strains of *Pseudomonas aeruginosa* isolated from canine otitis externa. *Vet. Dermatol.* **2019**, *30*, 145-150.

[62] (a) Yilmaz, V.T.; Icsel, C.; Batur, J.; Aydinlik, S.; Sahinturk, P.; Aygun, M. Structures and biochemical evaluation of silver(I) 5,5-diethylbarbiturate complexes with

bis(diphenylphosphino)alkanes as potential antimicrobial and anticancer agents, *Eur. J. Med. Chem*. **2017**, *139*, 901-916. (b) Nomiya, K.; Takahashi, S.; Noguchi, R. Synthesis and crystal structure of a hexanuclear silver(I) cluster $[Ag(Hmna)]_6 \cdot 4H_2O$ (H_2mna=2-mercaptonicotinic acid) and a supramolecular gold(I) complex $H[Au(Hmna)_2]$ in the solid state, and their antimicrobial activities. *J. Chem. Soc. Dalton Trans.* **2000**, 2091-2097. (c) Jaros, S.W.; Guedes da Silva, M.F.C.; Krol, J.; Oliveira, M.C.; Smolenski, P.; Pombeiro, A.J.L.; Kirillov, A.M. Bioactive Silver–Organic Networks Assembled from 1,3,5-Triaza-7-phosphaadamantane and Flexible Cyclohexanecarboxylate Blocks. *Inorg. Chem*. **2016**, *55*, 1486-1496. (d) Nomiya, K.; Kasuga, N.C.; Takayama, A. Synthesis, structure and antimicrobial activities of polymeric and nonpolymeric silver and other metal complexes, in: Munoz-Bonilla, A.; Cerrada, M.L.;, Fernandez-Garcia, M. (Eds.), Polymeric Materials with Antimicrobial Activity: from Synthesis to Applications, RSC Publishing, Cambridge, **2014**, pp. 156-207.

[63] Mohr, F.; Sanz, S.; Tiekink, E. R. T.; Laguna, M. Water-Soluble and Water-Stable Organometallic Gold(II) Complexes. *Organometallics* **2006,** *25,* 3084-3087.

[64] Sheldrick, G. M. *SHELXT*-Integrated space-group and crystal-structure determination. *Acta Cryst*. **2015**, *C71*, 3–8.

[65] Spek, A. L. Structure validation in chemical crystallography. *Acta Cryst*. **2009**, *D65*, 148–155.

[66] Holliday, D.L.; Speirs, V. Choosing the right cell line for breast cancer research. *Breast Cancer Res,* **2011**, *13*, 215-222.

[67] Knasmuller, S.; Mersch-Sundermann, V.; Kevekordes, S.; Darroudi, F.; Huber, W.W.; Hoelzl, C.; Bichler, J.; Majer, B.J. Use of human-derived liver cell lines forthe detection of environmental and dietary genotoxicants; current state of knowledge. *Toxicology* **2004**, *198*, 315–328.

[68] Tahara, H.; Matsuda, S.; Yamamoto, Y.; Yoshizawa, H.; Fujita, M.; Katsuoka, Y.; Kasahara, T. High-content image analysis (HCIA) assay has the highest correlation with direct counting cell suspension compared to the ATP, WST-8 and Alamar blue assays for measurement of cytotoxicity. *J Pharm Toxicol Methods* **2017**, *88*, 92-99.

[69] Repetto, G.; del Peso, A.; Zurita, J.L. Neutral red uptake assay for the estimation of cell viability/cytotoxicity. *Nat Protoc* **2008,** *3,* 1125-1131.

[70] CLSI. Performance Standards for Antimicrobial Susceptibility Testing. 29th ed. CLSI supplement M100. Wayne, P.A.: Clinical and Laboratory Standards Institute; **2019**.

[71] Palomino, J.C.; Martin, A.; Camacho, M.; Guerra, H.; Swings, J.; Portaels, F. Resazurin microtiter assay plate: simple and inexpensive method for detection of drug resistance in Mycobacterium tuberculosis. *Antimicrob Agents Chemother.* **2002,** *46*, 2720-2722.

Entry for the Table of Contents

New cationic silver(I) metallophosphazenes were obtained and characterised. The *in vitro* cytotoxic activity against two tumour human cell lines, MCF7 and HepG2, and antimicrobial activity against Gram-positive, Gram-negative and Mycobacteria strains were screened. Both IC_{50} and MIC values revealed that all the tested complexes showed outstanding biological activity.

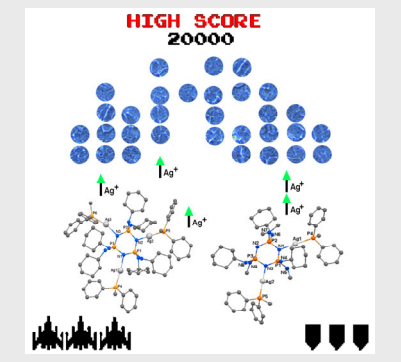

*E. Gascón, S. Maisanaba, I. Otal, E. Valero, G. Repetto, P.G. Jones, J. Jiménez**

(Amino)cyclophosphazenes as multisite ligands for the synthesis of antitumoral and antibacterial silver(I) complexes.